Critical Reviews in Biochemistry and Molecular Biology, 33(2):95–149 (1998)

Ribosomal tRNA Binding Sites: Three-Site Models of Translation

Nils Burkhardt, Ralf Jünemann, Christian M. T. Spahn, and Knud H. Nierhaus

Max-Planck-Institut für Molekulare Genetik, AG Ribosomen, Ihnestr. 73, D-14195 Berlin, Germany

ABSTRACT: The first models of translation described protein synthesis in terms of two operationally defined tRNA binding sites, the P-site for the donor substrate, the peptidyl-tRNA, and the A-site for the acceptor substrates, the aminoacyl-tRNAs. The discovery and analysis of the third tRNA binding site, the E-site specific for deacylated tRNAs, resulted in the allosteric three-site model, the two major features of which are (1) the reciprocal relationship of A-site and E-site occupation, and (2) simultaneous codon-anticodon interactions of both tRNAs present at the elongating ribosome. However, structural studies do not support the three operationally defined sites in a simple fashion as three topographically fixed entities, thus leading to new concepts of tRNA binding and movement: (1) the hybrid-site model describes the tRNAs' movement through the ribosome in terms of changing binding sites on the 30S and 50S subunits in an alternating fashion. The tRNAs thereby pass through hybrid binding states. (2) The α-ε model introduces the concept of a movable tRNA-binding domain comprising two binding sites, termed α and ε. The translocation movement is seen as a result of a conformational change of the ribosome rather than as a diffusion process between fixed binding sites. The α-ε model reconciles most of the experimental data currently available.

KEY WORDS: protein synthesis, elongation cycle, ribosome structure, neutron scattering, electron microscopy.

Abbreviations: **EM,** electron microscopy; **IEM,** immuno electron microscopy; **SAS,** small angle scattering; **SANS,** small angle neutron scattering; **XSAS,** X-ray small angle scattering; **PRE** state, pre-translocational elongation state of the ribosome; **POST** state, posttranslocational elongation state of the ribosome; **L1 to L36,** proteins of the large ribosomal subunit (50S); **S1 to S21,** proteins of the small ribosomal subunit (30S); **rRNA,** ribosomal RNA.

TABLE OF CONTENTS

I. INTRODUCTION

Protein synthesis is a key step in realizing the genetic information. In all living organisms this is performed by ribosomes. These translate the genetic information, which was previously transcribed from DNA to a messenger RNA, into the amino acid sequence of a protein. The substrates of a ribosome are not merely amino acids but aminoacylated tRNA molecules that fulfill two essential functions. First, they bring the amino acids in an activated form to the ribosome, because the amino acids are bound via phosphodiester bonds to the 3′-CCA ends of the tRNAs. The energy content of these chemical bonds is sufficient to allow peptide bond formation. Second, the tRNAs link the information coded in the nucleotide sequence of the mRNA into the amino acid sequence of the growing peptide. An essential prerequisite for this specific linkage is the correct aminoacylation of the tRNAs, which is performed by the aminoacyl-tRNA synthetases. One aminoacyl-tRNA synthetase exists for each amino acid (for exceptions see Ibba et al., 1997). Significant progress has been made in resolving the tRNA-synthetase interaction at the molecular level (for reviews see Cusack, 1995). In turn, the correct interaction of the ribosome with the tRNA is crucial for the selection of the aminoacyl-tRNA and for the maintenance of the reading frame. It follows that

an understanding of the functional and structural aspects of this interaction is of pivotal importance for an appropriate description of protein biosynthesis.

Ribosomes can dissociate into two subunits, each consisting of both proteins and ribosomal RNA (rRNA). Ribosomes from the three domains bacteria, eukarya and archea vary considerably in size and number of constituents (Wittmann, 1986). However, they exhibit a number of common features as reflected by the degree of sequence conservation of rRNAs and proteins (Noller, 1991; Wittmann-Liebold et al., 1990). The eubacterial ribosome from *E. coli* is the most extensively characterized to date. The small subunit (30S subunit) consists of 16S rRNA and 21 proteins (S1 to S21), the large subunit (50S subunit) contains two rRNA molecules (5S and 23S rRNA) and 33 different proteins (L1 to L36). The primary structure of all components is known (for reviews see Noller, 1991; Wittmann-Liebold et al., 1990). The total complex amounts to about 2.3 million Da, with a maximal diameter of 250 Å. Compared to ribosomes tRNA molecules are relatively small, with molecular masses ranging from 25.000 to 30.000 Da. They are highly modified molecules, L-shaped in three dimensions. The functional regions of the tRNA, namely, the anticodon and the acceptor ends located at the tips of the L-shape, are separated by approximately 75 Å.

Protein biosynthesis can be divided into three functional phases: initiation, elongation and termination. All three phases are guided and controlled by additional factors, that is, the initiation factors (IFs), the elongation factors (EFs) and the termination/release factors (RFs). The translation machinery ensures the accurate decoding of the messenger RNA (mRNA) leading to protein synthesis.

Translation initiation by bacterial ribosomes is primarily a function of the small ribosomal subunit together with three IFs (Gualerzi et al., 1990; Hartz et al., 1990). The 30S subunit binds mRNA in the presence of IF-1 and IF-3. The conserved Shine-Dalgarno sequence on the mRNA (located 7-12 nucleotides upstream of the start codon) base-pairs to the anti-Shine-Dalgarno sequence at the 3′-end of 16S rRNA. IF-2 together with GTP promotes the binding of fMet-tRNA$_f^{Met}$ to the start codon, usually AUG. This complex associates with a free 50S subunit to form a 70S ribosome, programmed with an mRNA and an fMet-tRNA$_f^{Met}$ at the ribosomal peptidyl site (P site). GTP is hydrolyzed on IF-2 and the factor is released from the initiation complex.

Elongation of the nascent peptide begins when an aminoacyl-tRNA enters the ribosome acceptor site (A site) in the form of a ternary complex aminoacyl-tRNA · EF-Tu · GTP. After GTP hydrolysis and dissociation of EF-Tu · GDP peptidyltransfer occurs. Completion of the cycle involves an EF-G-dependent translocation event, resulting in the movement of the peptidyl-tRNA from the A to the P site. EF-G is released after GTP hydrolysis.

The final step of protein synthesis is signaled by a stop codon in the A site and recognition by RF-1 (UAA, UAG) or RF-2 (UAA, UGA; Tate and Brown, 1992). A third factor RF-3 enhances the activity of RF-1 and RF-2 (Grentzmann et al., 1994; Mikuni et al., 1994; Freistroffer et al., 1997). The peptidyl-tRNA bond is hydrolyzed and the synthesized protein leaves the ribosome. The tRNAs and mRNA dissociate from the ribosome, which in turn dissociates into the two subunits. The last step is guided by EF-G and the ribosome recycling factor RRF (Janosi et al., 1996; Pavlov et al., 1997).

The kernel of translation is the elongation cycle. Its formal outline was thought to be understood more than 30 years ago (Watson, 1963, 1964; Lipmann, 1963). However, with the discovery of a third tRNA binding site, the E site, in addition to the classic A and P sites, it became evident that the classic two-

site model is incomplete (Rheinberger et al., 1981; Grajevskaja et al., 1982; Rheinberger and Nierhaus, 1983). It is clear now that the whole process is much more complex than originally believed. We still do not understand the basic principles of tRNA selection during the decoding process, the peptidyltransferase reaction, and the translocation at the molecular level. Nevertheless, several leaps have been made in recent times toward a detailed understanding of the elongation cycle. In this review we summarize the functional and structural achievements and critically discuss different three-site models reflecting the current views of elongation (for a detailed description of the functions of the ribosomal elongation factors see the recent review of Czworkowski and Moore, 1996).

II. CONCEPTS OF THE TRANSLATION PROCESS

A. From Two to Three Sites

In the early 1960s, Watson (1963, 1964) and Lipmann (1963) suggested similar models for the elongation cycle with two tRNA binding sites. Such models encompassed the minimal requirements of the peptidyltransferase reaction, that is, the existence of a binding site (P site) for the donor substrate peptidyl-tRNA, and a binding site (A site) for the acceptor substrate aminoacyl-tRNA. With the unraveling of the so-called puromycin reaction (Traut and Monroe, 1964), the two-site model became generally accepted. The antibiotic puromycin is a structural analogue of the aminoacyl end of an aminoacyl-tRNA. It can bind to the A-site region of the peptidyltransferase center and accepts the peptidyl residue from peptidyl-tRNA via formation of a peptide bond. This puromycin reaction should take place only if the peptidyl-tRNA is present in the P site, and not in the A site. Consequently, the site location of a peptidyl-tRNA is defined operationally by the puromycin reaction: a positive puromycin reaction indicates P-site location, whereas a negative puromycin reaction is evidence for an A-site location. It is clear that charged tRNAs only can be localized with the help of the puromycin reaction.

If the peptidyl-tRNA analogue AcPhe-tRNA^{Phe} is bound directly to poly(U) programmed ribosomes, it is reactive with puromycin, and thus is located in the P site. If a deacylated tRNA^{Phe} is bound to a poly(U) programmed ribosome followed by an AcPhe-tRNA^{Phe} to create a pretranslocational complex (PRE complex), the AcPhe-tRNA^{Phe} is bound to the A site, as indicated by a negative puromycin reaction. Therefore, the deacylated tRNA^{Phe} was thought to be in the P site, that is, to be in the same ribosomal binding site as the puromycin-reactive AcPhe-tRNA^{Phe} directly bound to vacant ribosomes. Although a puromycin reaction with an AcPhe-tRNA^{Phe} present at the A site was detected (Semenkov et al., 1992), the operational definition of the A site still holds, as this reaction is extremely slow (more than 200-fold slower than the corresponding P-site reaction; Semenkov et al., 1992; A. Potapov, C. M. T. Spahn, and K. H. Nierhaus, unpublished observation) and thus allows an unequivocal discrimination between an A- and P-site location of a peptidyl-tRNA.

In the beginning of the 1980s it was discovered that poly(U) programmed 70S ribosomes from *E. coli* can bind up to three molecules of deacylated tRNA^{Phe} (Rheinberger and Nierhaus, 1980; Rheinberger et al., 1981; Grajevskaja et al., 1982). As Phe-tRNA^{Phe} can occupy no more than two sites (Rheinberger et al., 1981), there must be a third ribosomal binding site in addition to the A and P sites, that exclusively accepts deacylated tRNA. The new site was termed the E site (E for exit)

according to an early suggestion by Wettstein and Noll (1965). Only the number of bound deacylated tRNAs could be determined in the course of a saturation experiment. For this site, localization with the puromycin reaction is unsuitable, as it requires a charged tRNA.

In order to determine the site location of the deacylated tRNA during a saturation experiment, an "indicator reaction" was developed. It is based on the addition of a small amount of Ac-aa-tRNA, whose site location can be followed as a function of the preoccupation state of the ribosome with deacylated tRNA. During occupation by the first deacylated $tRNA^{Phe}$ of poly(U) programmed 70S ribosomes, the indicator AcPhe-tRNA was shifted from the P to the A site, because $tRNA^{Phe}$ bound first to the P site as expected (Rheinberger et al., 1981). During occupation by the second tRNA the binding level of the indicator AcPhe-tRNA at 37°C was not affected. Only when the binding level of the deacylated $tRNA^{Phe}$ exceeded two does the subsequent AcPhe-tRNA binding decrease, showing that the E site is occupied before the A site (Rheinberger et al., 1981). In a more complete analysis the apparent association constant of AcPhe-tRNA was determined, dependent on the amount of pre-bound $tRNA^{Phe}$ (Rheinberger and Nierhaus, 1986a). The same picture was observed: a binding level of $tRNA^{Phe}$ between one and two per ribosome barley affected the association constant of AcPhe-tRNA to the A site (37°C). The association constant was strongly decreased after binding a third $tRNA^{Phe}$. Therefore, $tRNA^{Phe}$ occupies the binding sites of poly(U) programmed ribosomes in a sequential manner. First the P site is occupied, then the E site, and only at a high excess of tRNA the A site. Alternatively, if we assume that the second tRNA can bind either to the E site or to the A site, the cogant conclusion is that the affinity for the third tRNA is reduced compared with that of the second tRNA (Rheinberger et al., 1981; Schilling-Bartetzko et al., 1992a), and that the affinity of deacyl-tRNA for the E site is at least as high as for the A site and probably even higher (Schilling-Bartetzko et al., 1992a).

The existence of a third tRNA binding site was initially disputed (for review see Rheinberger, 1991), but later it could be confirmed by other groups (Grajevskaja et al., 1982; Kirillov et al., 1983; Lill et al., 1984). As there is now also structural evidence for the E site by cross-linking experiments (e.g., Wower et al., 1993a; Döring et al., 1994), footprinting experiments (Moazed and Noller, 1989a), neutron scattering (Nierhaus et al., 1998), and electron microscopy (Agrawal et al., 1996; Stark et al., 1997), the existence of three tRNA binding sites on *E. coli* ribosomes is now generally accepted. Moreover, three tRNA binding sites could be shown for ribosomes from the archeon *Halobacterium halobium* (Saruyama and Nierhaus, 1986), mammalian ribosomes from rabbit liver (Rodnina et al., 1988), and human placenta (Graifer et al., 1992), and yeast ribosomes from *Saccharomyces cerevisiae* (Triana-Alonso et al., 1995). A report of a fourth site, the S site on mammalian ribosomes (Rodnina and Wintermeyer, 1992) could not be confirmed (El'skaya et al., 1997). Thus, three tRNA binding sites seem to be a universal feature of the ribosome.

B. A Functional Model for the Elongation Cycle: the Allosteric Three-Site Model

The classic two-site model predicts that the ribosome in the pretranslocational state (PRE state) contains two tRNAs, a peptidyl-tRNA in the A site and deacyl-tRNA in the P site, but only one tRNA in the posttranslocational state (POST state), namely, a P-site

bound peptidyl-tRNA. In contrast, during poly(U) translation the ribosome binds 2.13 ± 0.06 tRNAs on average, although at least 70% of the ribosomes are in the POST state (Rheinberger and Nierhaus, 1983). Furthermore, in a translocation experiment an uncoupling of translocation and tRNA release was observed. The deacyl-tRNA remained on the POST-state ribosomes and could be even pelleted with the complex. For this, it was concluded that translocation of the peptidyl-tRNA from the A to the P site was accompanied by a co-translocation of deacyl-tRNA from the P to the E site (Rheinberger and Nierhaus, 1983).

If the deacyl-tRNA is not released from the ribosome during translocation, but rather is transferred and stably bound to the E site, there are three possibilities for release of the tRNA. It can be released during the next A-site occupation, during the following peptidyltransferase reaction, or during the immediately following translocation. The addition of the ternary complex was found to release the deacyl-tRNA from the E site (Rheinberger and Nierhaus, 1983). Because the addition of a ternary complex containing the non-cleavable GTP analogue GMP-PNP (preventing peptidyltransfer and dissociation of EF-Tu) induced the liberation of the E-site bound tRNA, the A-site occupation could be identified to be the trigger for the release (Rheinberger and Nierhaus, 1986a).

A corresponding release of deacyl-tRNA from the E site by the A-site ligand Phe-tRNA^{Phe} or AcPhe-tRNA^{Phe} could also be observed, when two deacyl-tRNAs were pre-bound to the P and E sites, respectively (Rheinberger and Nierhaus, 1986a). Interestingly, AcPhe-tRNA^{Phe} could bind in this case only at 37°C, but not at 0°C. Obviously, some activation energy is needed for a conformational change of the ribosome. Apparently, at low temperature, the occupied E site prevents the A-site ligand AcPhe-tRNA^{Phe} from binding. The ternary complex is the physiological A-site ligand and can even bind at 0°C, accompanied by a corresponding release of deacyl-tRNA, although with a lower binding efficiency than at 37°C. EF-Tu catalyzes the conformational change of the POST to PRE transition of the ribosome and thus allows A-site occupation also at low temperature.

If three tRNAs were pre-bound, the A-site binding of one equivalent of ternary complex was able to release two equivalents of deacyl-tRNAs from the ribosome (Rheinberger and Nierhaus, 1986a). This is an important control, because the site location of tRNAs with poly(U) as mRNA is always ambiguous and one could argue that tRNA release is due to chasing from the A site. If, however, one ternary complex releases two deacyl-tRNAs, only one can be removed by direct chasing from the A site, and the other must be removed from the E site by an indirect mechanism. A tRNA release triggered by an A-site occupation rather than by a translocation reaction could be also demonstrated in a system with a heteropolymeric mRNA (Gnirke et al., 1989). Because in that case unique codons were present at the A, P, and E sites, alternative explanations such as tRNA release after translocation and quantitative rebinding to the A site, or chasing of the E-site bound tRNA by a deacyl-tRNA contamination of the A-site ligand, could be ruled out.

These observations founded and substantiated the allosteric three-site model for the ribosomal elongation cycle (for reviews see Nierhaus, 1990; Rheinberger, 1991). Each tRNA passes through the ribosomal binding sites in the sequence A→P→E in the course of two elongation cycles. The A and E sites are coupled by a negative allostery. Occupation of either the A or E site lowers the affinity of the other site. Therefore, the elongating ribosome exists in two different conformations, each displaying two high-affinity tRNA binding sites, namely, A and P sites in the PRE state, and P and E sites in the

POST state. During elongation the ribosome oscillates between these two conformations. A schematic picture of an elongation cycle is depicted in Figure 1. An elongation cycle begins with the POST ribosome: the peptidyl-tRNA is bound at the P site and the deacyl-tRNA at the E site. A ternary complex encounters the low-affinity A site. A correct codon-anticodon interaction triggers the allosteric transition POST→PRE. As a consequence, the tRNA from the E site is released and the ternary complex now binds with high affinity. GTP is hydrolyzed by EF-Tu, and EF-Tu·GDP leaves the ribosome. This state with an aminoacyl-tRNA at the A position and a peptidyl-tRNA at the P position has a short lifetime, because peptidyltransfer takes place immediately. A peptide bond is formed, and the peptidyl-tRNA, extended by one amino acid, is bound at the A site. The deacyl-tRNA generated is bound at the P site. This PRE ribosome is the substrate for EF-G·GTP, which triggers the translocation reaction: the peptidyl-tRNA moves from the A to the P site and the deacyl-tRNA from the P to the E site. GTP is hydrolyzed and EF-G·GDP leaves the POST ribosome.

The allosteric three-site model distinguishes two types of A-site occupation, with respect to the occupation state of the E site. A-site occupation with a free E site occurs only in the first elongation cycle after initiation and is called A-site occupation of the i-type (i for initiation). All following A-site occupations are of the e-type (e for elongation) and occur on POST ribosomes with a filled E site. When AcPhe-tRNA^{Phe} was used as A-site ligand and the ribosome had one or two tRNA^{Phe} pre-bound to either the P site, or the P and E sites different activation energies were measured (Schilling-Bartetzko et al., 1992b). At 15 m*M* Mg^{2+} in a conventional buffer system (Table 1) the activation energy of the A-site occupation for the i-type was 47 kJ/mol and increased to 87 kJ/mol for the e-type. At a low Mg^{2+} concentration of 3 m*M* in a polyamine-containing buffer system (Table 1) the difference was even more pronounced. A-site occupation from the i-type showed an activation energy of 40 kJ/mol, while the activation energy for the e-type was 118 kJ/mol.

The allosteric three-site model provides a framework, within which the action of several antibiotics can be better understood (Hausner et al., 1988; for reviews see Spahn and Prescott, 1996). Aminoglycoside antibiotics, including streptomycin, hygromycin B, kanamycin A, and gentamycin C, all bind close to the decoding center of the ribosome. Although exibiting different interference patterns (e.g., only hygromycin and neomycin inhibit translocation), they are all in accord in blocking the A-site binding of the e-type. If the E site is free (A-site occupation of the i-type), only small effects are observed. Similarly, the translocation inhibitors viomycin and thiostrepton interfere strongly with A-site occupation of the e-type but have only a negligible effect on A-site occupation of the i-type.

The features of the allosteric three-site model have been demonstrated also with ribosomes from organisms other than *E. coli*, viz., ribosomes from both the archaeon *H. halobium* (Saruyama and Nierhaus, 1986) and the yeast *S. cerevisiae* (Triana-Alonso et al., 1995). Moreover, in the latter system the role of the elongation factor EF-3 could be clarified. EF-3 is a ribosome-dependent ATPase, unique and essential in higher fungi (for reviews see Triana et al., 1993, and references therein). An exceptionally strong difference between A-site occupations of the i- and e-types was observed. A-site occupation of the i-type was possible without EF-3, whereas in the case of a filled E site (e-type) a ternary complex could not bind to the A site, thus strikingly demonstrating the reciprocal linkage between the A and E sites. EF-3 and ATP were necessary for efficient ternary complex binding. Because EF-3 enhances chasing of

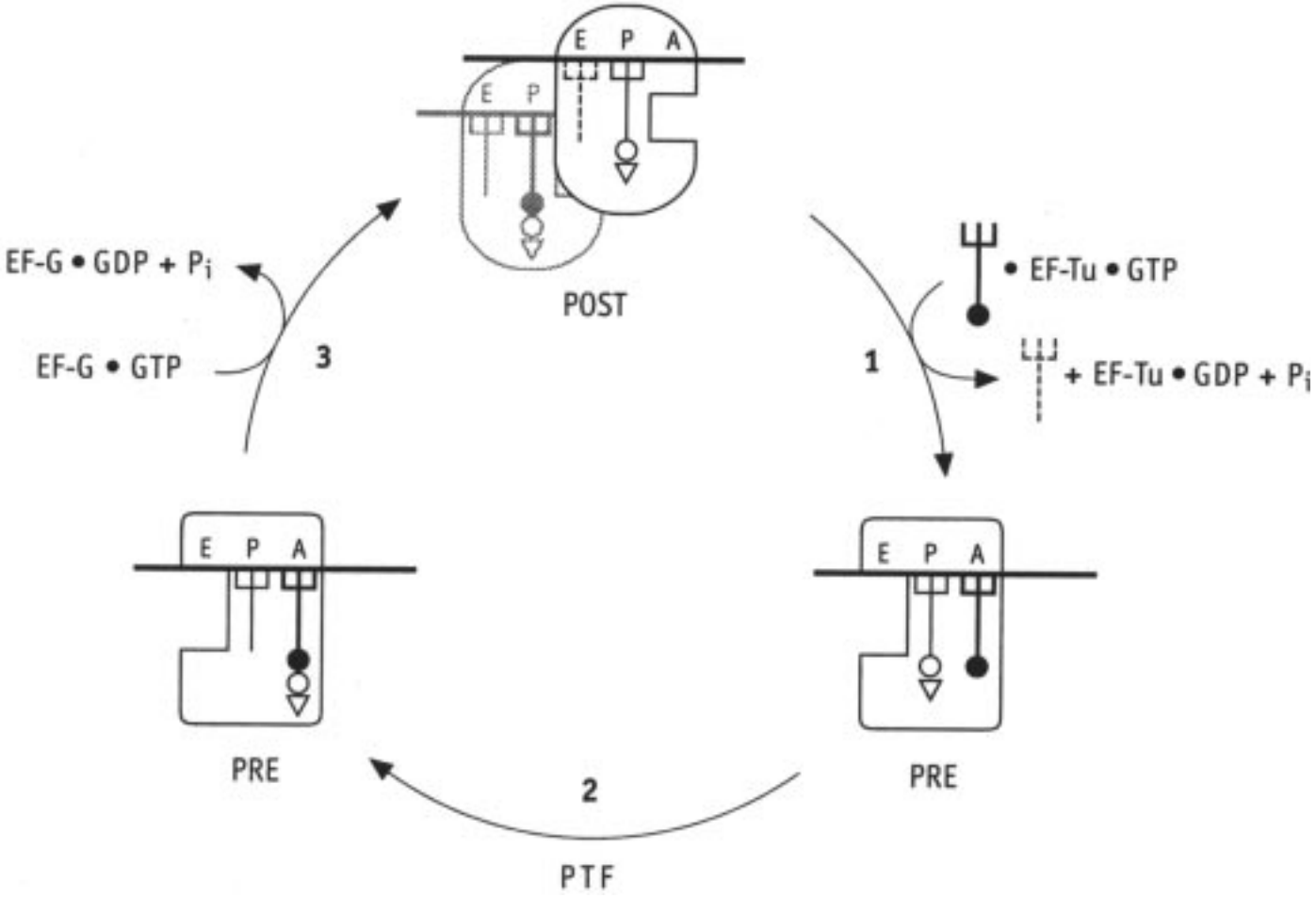

FIGURE 1. The allosteric three-site model for the elongation cycle. 1, A-site occupation; 2, peptidyltransfer (PTF); 3, translocation. (Adapted from Nierhaus, 1990.)

TABLE 1
Concentrations of Ions and Polyamines Important for Ribosomal Functions *In Vitro* in Various Buffer Systems and *In Vivo*

	Mg^{2+} [mM]	K^+, NH_4^+ [a] [mM]	Polyamines [mM]		
			spermd.	sperm.	putr.
Conventional system[e]	7–20	100	None	None	None
Polyamine system[f]	3–6	150	2[b]	0.05[b]	None[c]
In vivo[g]	~4 (free Mg^{2+})	~150	1–4	~0.03[d]	20[c]

Note: sperm., spermine; spermd., spermidine; putr., putrescine.

[a] K^+ and NH_4^+ are nearly equivalent in *in vitro* systems of protein synthesis due to their similar ionic radii.
[b] We used 0.4 m*M* spermidine and 0.6 m*M* spermine before 1990. 2 m*M* spermidine and 0.05 m*M* spermine were found to achieve the same results concerning rate, accuracy, and active fraction. Therefore, we have preferred the latter concentration set since 1990, due to their correlation with the corresponding *in vivo* data.
[c] Putrescine has no effects on protein synthesis *in vitro* as have additions of cadaverine and agmatine (B. Lewicki and K. H. Nierhaus, unpublished) that also are present in significant amounts *in vivo.*
[d] 1/100 the concentration found for spermidine; Kamekura et al. (1987).
[e] Semenkov et al. (1996).
[f] Rheinberger and Nierhaus (1987); Bartetzko and Nierhaus (1988).
[g] Lusk et al. (1968); Tabor and Tabor (1985); Kamekura et al. (1987).

the E-site bound tRNA in an ATPase-dependent manner, EF-3 was termed an E-site factor as it helps to release the E-site bound tRNA during the A-site occupation (Triana-Alonso et al., 1995).

C. Properties of the E Site

It is generally accepted that tRNA is not directly released from the P site during translocation but is transferred to the E site (Nierhaus, 1990; Wintermeyer et al., 1990). Disagreement exists on several points concerning the properties of the E site, that is, the stability of the E-site bound tRNA and the importance of the codon-anticodon interaction (e.g., Rheinberger, 1991; Nierhaus, 1993; Wintermeyer et al., 1990; Semenkov et al., 1996). Furthermore, the importance of the E site is disputed. Wintermeyer and coworkers favor the view that the E site only facilitates the release of deacylated tRNA from the P site in the course of the translocation reaction, whereas Nierhaus and colleagues assign a prominent role to the E-site bound tRNA and suggest a reciprocal interaction between A and E sites. In the following section we review this issue.

1. Stability of the E-Site Bound tRNA

The affinity of the E site for deacyl-tRNA was estimated to be around $1 \times 10^7\ M^{-1}$

(Rheinberger et al., 1981; Schilling-Bartetzko et al., 1992a). Wintermeyer and co-workers could also confirm the existence of the E site (Lill et al., 1984), although they initially ruled out that a third tRNA binding site could be stronger than $5 \times 10^5\ M^{-1}$ (Wintermeyer and Robertson, 1982). Dependent on the buffer conditions they found the binding constant for the E site to be $0.4 \times 10^7\ M^{-1}$ to $4 \times 10^7\ M^{-1}$ (Lill et al., 1986). There is no contradiction concerning the binding constants, that is, in the binding energy and the binding stability in a thermodynamic sense. In order to test the site location of deacyl-tRNA, Lill et al. (1984) used an "indicator reaction" similiar to that of Rheinberger et al. (1981), in which the binding of AcPhe-tRNA^{Phe} or of a ternary complex was exploited to measure the availability of the P and A sites. In agreement with Rheinberger et al. (1981), they confirmed a sequential binding. First the P site was occupied and then the E site, prior to, or concomitantly with, the A site (Lill et al., 1984). In contrast, the A site was occupied as the second site in a heterologous system with *E. coli* ribosomes and yeast tRNA. Furthermore, E-site binding could be detected by nitrocellulose filtration only when the sample was spotted directly on the filter, whereas E-site binding of the homologous tRNA^{Phe} from *E. coli* could be detected also by filtration with prior dilution, at least at Mg^{2+} concentrations of 15 m*M* and above (Lill et al., 1984). This demonstrates that results obtained with a heterologous system may not be valid for the homologous situation.

Despite the agreement in the association constant of the E site, differences in the amount of E-site bound tRNA after translocation were reported. Nierhaus and colleagues observed that only little deacyl-tRNA was released when translocated from the P to the E site (e.g., Rheinberger and Nierhaus, 1983, 1986a; Gnirke et al., 1989). In contrast, Wintermeyer and colleagues observed a significant release of the deacyl-tRNA after translocation under equilibrium conditions (Robertson et al., 1986; Robertson and Wintermeyer, 1987; Semenkov et al., 1996). Obviously, different kinetic stabilities of the E-site bound tRNA account for the different binding levels in the enzymatically derived POST state. Three main factors give rise to this discrepancy: (1) the source of the tRNA, (2) the preparation of ribosomes, and (3) the buffer conditions.

1. In some studies a heterologous system was used to exploit the fluorescent properties of yeast tRNA or some derivatives of yeast tRNA in the presence of *E. coli* ribosomes (e.g., Robertson et al., 1986; Robertson and Wintermeyer, 1987). However, the affinity of yeast tRNA for the E site is approximately one order of magnitude lower than that of *E. coli* tRNA (Lill et al., 1986).
2. The preparation of ribosomes can also influence the stability of the E-site bound tRNA. Ribosomes isolated under low-salt conditions (Rheinberger et al., 1988) have a more stable E site than high salt-washed ribosomes (Robertson et al., 1984; Robertson and Wintermeyer, 1987). Washing the 70S ribosomes with, for example, 500 m*M* NH_4Cl is a step of the ribosome isolation procedure by Wintermeyer and others intended to remove impurities from the ribosome. Such a procedure has the drawback that it can partially remove up to 14 ribosomal proteins (Gnirke et al., 1989) and thus gives rise to a heterogeneous population of ribosomes.
3. The buffer composition is important concerning the occupation of the E-site after a translocation step. Standard systems for *in vitro* translation or for preparation of ribosomal complexes contain mainly Mg^{2+} as divalent cations and K^+/NH_4^+ as monovalent cations. The optimal Mg^{2+}

concentration for poly(U) dependent poly(Phe) synthesis is 10 to 12 m*M* at 150 m*M* NH_4^+ (Chinali and Parmeggiani, 1982; Bartetzko and Nierhaus, 1988). Lowering the Mg^{2+} concentration leads to an increasing loss of the deacyl-tRNA during the translocation reaction (Robertson et al., 1984; Robertson and Wintermeyer, 1987). At 20 m*M* or 15 m*M* Mg^{2+} most of the tRNA stayes on the ribosome, whereas the E-site affinity at 4 mM Mg^{2+} is estimated to be below $4 \times 10^5\ M^{-1}$. The Mg^{2+} concentration is around 4 m*M* *in vivo* (Lusk et al., 1968; Table 1). However, the results obtained in standard buffer systems cannot be extrapolated to the *in vivo* situation, because a low Mg^{2+} concentration produces additional effects beyond inactivation of the E site. It was found that the overall poly(U) directed Phe incorporation as well as the extent of tRNA binding to P and A sites decreases in a manner parallel to the inactivation of the E site, when the Mg^{2+} concentration is lowered below 10 m*M* (Rheinberger and Nierhaus, 1987). Thus, conventional buffer systems (Table 1) are not sufficient to mimic the environment of the ribosome within a cell and to allow protein synthesis to proceed with *in vivo*-like characteristics in terms of speed and accuracy. Especially important for protein biosynthesis at physiologic Mg^{2+} concentration is the presence of polyamines, which are found in the cytosol (Tabor and Tabor, 1985; Kamekura et al., 1987; see Table 1).

Two polyamine-containing buffer systems have been described that allow poly(U) directed poly(Phe) synthesis to be performed at a rate and accuracy close to the corresponding *in vivo* values: the polymix system (Jelenc and Kurland, 1979), and the less complex polyamine system (Bartetzko and Nierhaus, 1988; see Table 1). A complete uncoupling of translocation and tRNA release could be observed in the latter system with a Mg^{2+} concentration of 6 m*M*, or even 3 m*M* (Rheinberger and Nierhaus, 1987). Recently, the lack of tRNA release after translocation in the polyamine system could be confirmed even with salt-washed ribosomes, whereas a nearly complete release was observed with conventional buffer systems at 7 m*M* Mg^{2+} (Table 1; Semenkov et al., 1996). An almost complete, albeit slower, release was also seen in the polymix system. Therefore, it is clear that the release of the deacyl-tRNA after translocation from the P to the E site strongly depends on the buffer system. Note that the polyamine system closely matches the *in vivo* concentrations of monovalent cations, Mg^{2+}, spermine, and spermidine (see Table 1).

The question of whether a deacylated tRNA is bound at the E site in a stable fashion *in vivo* is considered below. The allosteric three-site model predicts that the POST state contains two occupied high-affinity tRNA binding sites, the P site and the E site. The stability of the E site was deduced from the lack of tRNA release after translocation (e.g., Rheinberger and Nierhaus, 1983; Rheinberger and Nierhaus, 1986a; Gnirke et al., 1989). Because the E-site occupation was observed under equilibrium conditions, it reflects *thermodynamic* stability. In contrast, Wintermeyer and co-workers have stated that a tRNA at the E site is bound in a *kinetically* labile fashion and dissociates passively from the ribosome during the translocation reaction and *before* A-site occupation occurs (Robertson et al., 1986; Robertson and Wintermeyer, 1987). In this view the E-site bound tRNA characterizes a short-lived kinetic intermediate of the translocation reaction. These authors' argument is based on the observations that the E-site bound tRNA dissociates rapidly from the POST ribosome and can be easily

chased with a large excess of non-labeled deacyl-tRNA. Furthermore, a low stability was seen by nitrocellulose filtration with prior dilution of the sample, especially when yeast deacyl-tRNA was used or a Mg^{2+} concentration below 15 m*M* (Lill et al., 1984). In contrast, under the conditions of the polyamine system (Table 1) the E-site bound tRNA was kinetically stable enough to survive nitrocellulose filtration with prior dilution. Furthermore, the POST complex could be pelleted by centrifugation and resuspended without significant loss of deacyl-tRNA (Gnirke et al., 1989). During this procedure the POST complex was treated at far from equilibrium conditions for several hours, albeit at low temperature. A higher chaseability of the E-site bound tRNA when compared with that of A- or P-site bound tRNAs was also observed by Nierhaus and co-workers (Rheinberger and Nierhaus, 1986b; Rheinberger et al., 1986). If the chaseability is defined as kinetic lability, then tRNA binding at the E site is labile indeed. However, the relevant biochemical question is not whether the E-site bound tRNA can be chased, but rather whether the dissociation of the tRNA from the E site occurs fast enough to proceed passively (i.e., without involvement of an allosteric mechanism) within one elongation cycle.

The dissociation rate constant for the E site was measured to be 0.5 s^{-1} or 0.1 s^{-1}, and the speed of poly(Phe) synthesis was given to be 5 s^{-1} under the same conditions (Robertson et al., 1986). According to these data the E-site bound tRNA remains on average for 2 to 10 s on the ribosome, a time sufficient for 10 to 50 elongation cycles. It follows that within 0.2 s, the time needed for one elongation cycle, only 2 to 10% of the E-site located tRNA could be released by passive diffusion. Therefore, the kinetic data reported by Wintermeyer and colleagues argue against a release of tRNA before A-site occupation and imply that the E site is occupied during A-site occupation, as proposed by the allosteric three-site model (Figure 1). This consideration suggests that an active mechanism for tRNA release is required. We note that the values mentioned previously represent a lower limit for the kinetic E-site stability. A higher E-site occupation is seen after translocation in the polyamine system (Table 1; Rheinberger and Nierhaus, 1987; Semenkov et al., 1996) and is evidently caused by a lower off-rate. This tendency contrasts with the faster rate of poly(Phe) synthesis per ribosome in this buffer system (Bartetzko and Nierhaus, 1988).

The situation *in vivo* is even more pronounced. The speed of protein biosynthesis is 20 amino acids per second (Dennis and Bremer, 1974), that is, the deacyl-tRNA must fall off the ribosome within 50 ms. There is practically no pool of deacyl-tRNA inside the cell, and therefore no equilibrium of E-site occupation can be established. A similar non-equilibrium situtation was realized *in vitro*, by the addition of aminoacyl-tRNA synthetase, which resulted in an increased release of deacylated tRNA after translocation (Robertson and Wintermeyer, 1987). If this scenario properly reflects the *in vivo* situation, that is, the tRNA binds only transiently to the E site and falls off the ribosome during translocation, it should not be possible to isolate POST polysomes containing an occupied E site. However, in fact at least 75% of the POST ribosomes *in vivo* carry a deacylated tRNA (Remme et al., 1989). Moreover, E-site specific protections of 23S rRNA are found in polysomes, also arguing for an occupied E site (Brow and Noller, 1983; Moazed and Noller, 1989a). Also, Wintermeyer and colleagues reported an occupied E site in native disomes after an incubation with EF-G for 10 min at 37°C at 6 m*M* Mg^{2+} without polyamines (Stark et al., 1997). The E-site bound tRNA is not released, even under these conditions that result in a very labile E site *in vitro* (Robertson et al., 1986; Rheinberger and Nierhaus, 1987). It follows that the E sites of POST-state ribosomes are stably occupied *in vivo*.

2. Codon-Anticodon Interaction at the E Site

In the absence of mRNA no more than one deacyl-tRNA could be bound to the ribosome, that is, at the P site, whereas in the presence of cognate mRNA the E and A sites could also be occupied (Rheinberger et al., 1981). This was taken as evidence that there is a codon-anticodon interaction at the E site. In contrast, other groups reported deacyl-tRNA binding to the P and E sites of unprogrammed ribosomes (Kirrilov et al., 1983; Lill et al., 1984).

A possible explanation is the difference in the filtration technique applied; for example, Lill et al. (1984) filtered the sample without prior dilution, applied a low vacuum during the filtration process, and could therefore also detect binding sites with lower affinity. In any case, the observation of a binding to unprogrammed ribosomes is not an argument against codon-anticodon interaction, as, for example, the P site of unprogrammed ribosomes can be occupied, however, codon-anticodon interaction at the P site is a well-established fact in the presence of a cognate codon (Lührmann et al., 1979; Peters and Yarus, 1979; Wurmbach and Nierhaus, 1979; Ofengand and Liou, 1981).

To investigate codon-anticodon contacts more carefully, two strategies were used: (1) direct binding of cognate vs. non-cognate tRNA, and (2) chasing of labeled bound tRNAs by an excess of unlabeled cognate or non-cognate tRNAs. In the case of poly(U) programmed ribosomes, only $tRNA^{Phe}$ could quantitatively fill the E site, whereas negligible binding was seen with the non-cognate $tRNA^{Lys}$ (Rheinberger et al., 1986). If poly(A) was used as template the opposite binding behavior of the tRNAs was seen: the cognate $tRNA^{Lys}$ quantitatively filled the E site, while the non-cognate $tRNA^{Phe}$ exhibited a low binding level. A similar influence of the codon on the binding of deacyl-tRNA to the E site was observed with a heteropolymeric mRNA (Gnirke et al., 1989).

In addition, chasing experiments also revealed an interaction between codon and anticodon in the E site (Rheinberger et al., 1986; Rheinberger and Nierhaus, 1986b). In poly(U) and poly(A) systems the corresponding chasing efficiencies were particularly pronounced: when cognate instead of non-cognate chasing substrates were applied, the difference was larger than one order of magnitude, as revealed by the chasing factor. The chasing factor was defined as the amount of labeled tRNA chased by the cognate competitor divided by the amount chased by the non-cognate one (Rheinberger and Nierhaus, 1986b; note that the chasing factor so defined is not equal to the ratio of the affinities). A more exhaustive analysis by Lill and Wintermeyer (1987) led in principle to similar figures. At 20 m*M* Mg^{2+} they found on average a 4-fold stabilization of binding to the E site by codon-anticodon and at 10 m*M* Mg^{2+} even a 20-fold stabilization, with a maximum of about 45-fold. At 10 mM Mg^{2+} the ratio of the affinity constants between the cognate $tRNA^{Phe}$ and near-cognate tRNAs was on average 11 when two basepairs could be formed between codon and anticodon of the near-cognate tRNA in the E site, 24 with one basepair, and 35 when a basepair could not be formed. It follows that the codon-anticodon interaction significantly contributes to the binding affinity at the E site (Lill and Wintermeyer, 1987). However, these authors stated that the contribution of the codon-anticodon interaction to E-site binding is much smaller than its contribution to binding to the A or P sites. Nierhaus and colleagues have not quantified the influence of codon-anticodon in terms of affinity (Rheinberger and Nierhaus, 1986b; Rheinberger et al., 1986), but in their experimental system the influence of codon-anticodon interaction is

higher than that measured by Lill and Wintermeyer (1987). This follows from a comparison of the chasing abilities of $tRNA^{Phe}$ compared with $tRNA^{Lys}$ in a experiment with poly(A) as mRNA. $tRNA^{Lys}$ is among the tRNAs having a very low intrinsic affinity for a non-programmed ribosome, whereas $tRNA^{Phe}$ exhibits a strong intrinsic affinity (Lill and Wintermeyer, 1987; Gnirke et al., 1989). However, in the poly(A) system efficient chasing of labeled $tRNA^{Lys}$ from the E site occurs only with the cognate $tRNA^{Lys}$ and not with the non-cognate $tRNA^{Phe}$ (Rheinberger and Nierhaus, 1986b; Rheinberger et al., 1986). We note that even a weak codon-anticodon interaction is difficult to explain by structural models, in which the anticodon has been described as distant from the codon (Agrawal et al., 1996; Stark et al., 1997).

In line with the importance of codon-anticodon interaction is the observation that a cross-link between an E-site located $[2N_3A76]tRNA^{Phe}$ and the 23S rRNA could be found only when the $tRNA^{Phe}$ was cognate for the E-site codon (Wower et al., 1995). Accordingly, no cross-link to the 23S rRNA was found when $tRNA^{Phe}$ was bound to poly(A) programmed ribosomes (Wower et al., 1993a). Wintermeyer and co-workers have found that an intact 3′-CCA end is an essential feature for the specific binding of deacyl-tRNA to the E site and is important for efficient translocation from P to E site (Lill et al., 1989). The cross-linking studies (Wower et al., 1993a; Wower et al., 1995) imply that the 3′-CCA end is in different positions, dependent on the presence or absence of codon-anticodon interaction. A proper contact of the 3′-CCA end with its ribosomal binding site might therefore require codon-anticodon interaction.

It has been speculated that two continuous codon-anticodon interactions in the A and P sites in the PRE state and in the P and E sites in the POST state are involved in the stable fixation of the mRNA (Rheinberger and Nierhaus, 1983). This hypothesis has been questioned, one argument being that disruption of codon-anticodon interactions takes place during translocation from the P to the E site (Kirillov and Semenkov, 1986), and the other, that codon-anticodon interactions might be too weak and take place only transiently (Lill and Wintermeyer, 1987). A recent report supports the importance of codon-anticodon interaction *in vivo* (Horsfield et al., 1995): a common source for (–1)frameshifts are so-called slippery sequences of seven nucleotides within the translatable region of mRNAs. Previously it was thought that these frameshifts occur in the PRE state of the ribosome with a simultaneous slippage of A- and P-site bound tRNAs. In contrast, Horsfield et al. (1995) have shown that such a frameshift event takes place in the POST state. The fact that the slippery sequence comprises seven nucleotides provides evidence for the existence of codon-anticodon interaction at the E site *in vivo*; in the absence of such an interaction, the slippery sequence would consist of four instead of seven nucleotides. Obviously, the possibility of codon-anticodon interaction must be maintained even after the frameshift in order to allow frameshift to occur. This implies that codon-anticodon interaction at the E site should be involved in the maintenance of the reading frame, as proposed previously (Rheinberger et al., 1986). Furthermore, this observation indicates that E-site binding *in vivo* is more stable than expected from a mere kinetic intermediate (see Section II.C.1).

3. Reciprocal Coupling between A and E Sites and Implications for Accuracy of Decoding

The allosteric three-site model proposes a process of at least two steps for the A-site occupation during elongation. In the POST state of the ribosome the A site has low

affinity for ternary complexes. Recognition of codon-anticodon occurs at the low-affinity A site (first step) and a successful recognition induces a conformational change of the ribosome (second step). As a result the affinity for the E-site bound deacyl-tRNA is reduced and the tRNA leaves the ribosome, while the aminoacyl-tRNA is bound with high affinity at the A site. Such a mechanism has implications for the accuracy of tRNA selection (Nierhaus, 1993). The principle of such a two-step A-site occupation had already been proposed by Ninio (1974). Principally, mainly codon-anticodon interaction should contribute to the binding energy at the A site in its low-affinity state, in contrast to the high-affinity state, in which contacts between the whole ternary complex, including EF-Tu, and the ribosome can also contribute to the binding energy. Note that the presence of EF-Tu within the ternary complex increases the affinitiy for the A site by more than two orders of magnitude as compared to naked aminoacyl-tRNA (Schilling-Bartezko et al., 1992a). All such contacts, apart from codon-anticodon interaction, are non-discriminatory, that is, they are essentially the same for the cognate ternary complexes and for the non-cognate ones. In a high-affinity A site these non-discriminatory contacts will slow the dissociation of the non-cognate ternary complexes. Subsequent steps of the elongation cycle must be slow enough to allow the dissociation of incorrectly bound ternary complexes. However, if decoding takes place on a low-affinity A site, dissociation will be fast, and the subsequent steps can also proceed faster.

The discrimination energy $\Delta\Delta G$ between incorrect and correct substrates will be unchanged, regardless of whether reciprocal coupling between A and E sites exists. Therefore, such a mechanism cannot improve the accuracy beyond what would be expected from the thermodynamic mechanism, but rather reduce the time that is needed to exploit the discrimination energy. Such a mechanism is principally compatible with ribosomal proofreading. The idea of ribosomal proofreading started from the observation that the stability of codon-anticodon interactions of appropriate tRNAs could explain an accuracy of the decoding process of little better than 1/10 (i.e., one error per 10 incorporations; Grosjean et al., 1978), whereas an accuracy of about 1/1000 is observed *in vivo*. Therefore, it was suggested that the accuracy potential of codon-anticodon interaction must be exploited more than once (for reviews see Kurland et al., 1990). Kinetic proofreading can provide an accuracy that is higher than the thermodynamic limit by coupling the reaction to an energy-supplying reaction such as GTP cleavage: in this case, EF-Tu-dependent cleavage of GTP (Hopfield, 1974; Ninio, 1975). The increased GTP consumption observed during the incorporation of near-cognate amino acids was taken as a proof for the existence of a proofreading mechanism. However, alternative explanations exist (Nierhaus, 1990, and references therein). Furthermore, the determination of the crystal structure of a ternary complex aminoacyl-tRNA·EF-Tu·GTP revealed that EF-Tu interacts with the tRNA about 50 Å away from the anticodon at the T and acceptor stems (Nissen et al., 1995), which provides no simple explanation as to how EF-Tu and the EF-Tu-dependent cleavage of GTP could fulfill a possible proofreading function.

An alternative concept has been suggested, according to which the ribosomal decoding center recognizes the correctness of the stereochemistry of the partial Watson-Crick structure formed by codon-anticodon interaction (Potapov, 1982) rather than "sensing" the stability of codon-anticodon interaction several times. This alternative concept can explain the observation that a desoxyribo-codon at the A site severely interferes with A-site binding, although the mere stability of codon-anticodon interaction is virtu-

ally unchanged by the removal of the 2′-OH groups (Potapov et al., 1995). Furthermore, DNA polymerases use a stereochemical recognition mechanism (Echols and Goodman, 1991) and can achieve an accuracy of 10^{-5} without proofreading, although the stability of a correct base pair *versus* an incorrect one can only account for an accuracy of 10^{-1} to 10^{-2}.

More recently, a two-step mechanism for A-site occupation was also proposed by Powers and Noller (1994a,b). Based on protection of bases in the 16S rRNA, they inferred that the 530 loop might exist in two conformations, an open one with low affinity for EF-Tu·GTP and a closed one with high affinity. Successful recognition of codon-anticodon interaction shifts the conformation from the open to the closed conformation, and EF-Tu·GTP is consequently bound with high affinity. According to their model, a low-affinity A site does not require an occupied E site. Furthermore, ribosomes carrying only AcPhe-$tRNA^{Phe}$ in the P site exist in two different conformations, as evident from the differential effects of puromycin, tetracycline, viomycin and thiostrepton on two subpopulations of ribosomes (Kutay et al., 1990). Finally, even the empty ribosome can adopt two different conformations, one resembling the PRE, the other the POST conformation, as judged by synergistic effects of EF-Tu and EF-G on their respective uncoupled GTPases (Mesters et al., 1994). The allosteric three-site model suggests that tRNA-binding to the E site shifts the equilibrium toward the low-affinity A site due to the reciprocal interaction between these sites and can therefore have an effect on tRNA selection. Indeed, it has been found that ribosomes with an occupied E site discriminate much better against non-cognate ternary complexes than do ribosomes with an empty E site (Geigenmüller and Nierhaus, 1990). Correct codon-anticodon interaction in the E site is necessary for this effect, because a near-cognate deacyl-tRNA in the E site did not improve accuracy.

Recently, Semenkov et al. (1996) considered "the allosteric three-site model of elongation untenable". Repeating several of their older findings, albeit in a more defined system with a heteropolymeric mRNA, they interpreted some of their data as evidence against the existence of stable E-site binding and of negative cooperativity between E and A sites. Furthermore, they claimed that none of the features of the allosteric three-site model "withstood experimental scrutiny in other laboratories". The latter statement is incorrect, because Semenkov et al. (1996) have confirmed stable E-site binding in the polyamine system (Table 1) and have neglected *in vivo* observations that support stable binding and codon-anticodon interaction at the E site (Nierhaus et al., 1997; see also Sections II.C.1. and II.C.2.).

In the following we concentrate on discussing the crucial experiment (Figure 4 in Semenkov et al., 1996), which was thought to disprove the allosteric three-site model. Semenkov et al. (1996) constructed a POST complex in the polyamine buffer system (Table 1). fMet-[^{14}C]$tRNA_f^{Met}$ was bound to the P site of ribosomes that were programmed with an MFF-mRNA carrying the three defined codons AUG-UUU-UUC in the middle. In the next step [^{3}H]Phe-$tRNA^{Phe}$·EF-Tu·GTP was added. After an EF-G-dependent translocation, EF-G was removed. The deacylated [^{14}C]$tRNA_f^{Met}$ was translocated to the E site, where it remained quantitatively bound during the following manipulations. Thus, the $tRNA_f^{Met}$ was stably bound at the E site in agreement with the allosteric three-site model. Finally, a second ternary complex [^{3}H]Phe-$tRNA^{Phe}$·EF-Tu·GTP was quantitatively bound to the A site, while most of the $tRNA_f^{Met}$ remained at the E site. The binding of three tRNAs simultaneously was considered to disprove the allosteric three-site model.

However, the allosteric three-site model does in fact allow the binding of three tRNAs simultaneously in the POST state: a deacylated tRNA at the E site, a peptidyl-tRNA at

the P site, and an aminoacyl-tRNA at the low-affinity A site during the decoding process (Geigenmüller and Nierhaus, 1990). This state probably exists as a short-lived intermediate during the decoding process. The hybrid-site model (Moazed and Noller, 1989b) also allows the binding of three tRNAs for a POST ribosome: a deacylated tRNA at the E site, a peptidyl-tRNA at the P/P site, and an aminoacyl-tRNA within a ternary complex at the A/T site. A similar although not identical case was described in an experiment, in which the programmed ribosomes were saturated with deacylated tRNAs. The first tRNA occupied the P site and the second the E site, thus establishing the POST state, to which a third tRNA could be bound only in the presence of a high excess of tRNAs (Rheinberger et al., 1981), thus indicating a low-affinity state of the A site (Schilling-Bartetzko et al., 1992a). In contrast, only two tRNAs can be bound to ribosomes in the PRE state according to both models. A deacylated tRNA at the P site and a peptidyl-tRNA at the A site prevent the binding of a third tRNA to the E site (reciprocal linkage; allosteric three-site model). Similarly, the hybrid-site model predicts a peptidyl-tRNA at the A/P site and a deacylated tRNA at the P/E site leaving no site for a third tRNA. Therefore, the critical question concerning the experiment described by Semekov et al. (1996) is, whether a ribosome, carrying three tRNAs, is in the PRE or in the POST state. However, this question cannot be answered, because Semenkov et al. did not include appropriate controls, revealing the state of the ribosome. A peptide analysis—in order to demonstrate a quantitative tripeptide formation indicative for a PRE state—was not shown. Furthermore, a puromycin reaction as control was only performed before, and not after, the addition of the ternary complex (Semenkov et al., 1996), leaving undetermined the A- or P-site location of the peptidyl-tRNA. Therefore, no conclusion can be derived either in favor of or against the allosteric three-site model. However, following the interpretation of the authors, the experiment argues not only against the allosteric three-site model, but also against the hybrid-site model with the same stringency; this point was not considered by the authors (for further discussion see Nierhaus et al., 1997).

Some evidence for the reciprocal interaction between A and E sites can also be extracted from *in vivo* studies. Native polysomes contain on average 1.9 tRNAs per ribosome, and about 40% of the ribosomes are in the PRE and 60% in the POST state (Remme et al., 1989). In the case of labile E-site binding, 1.4 tRNAs would be expected to be on the ribosome, whereas in the case of stable E-site binding in the absence of a reciprocal interaction up to 2.4 tRNAs would be expected per ribosome. The observed number 1.9 therefore implies that two high-affinity sites are always present on the elongating ribosome. A second line of evidence comes from a study of tRNA mutations. It is known that a base substitution at the universal 3′-CCA end of tRNAs weakens the affinity of the tRNA for the E site (Lill et al., 1989). An analysis of the *in vivo* effects of a $tRNA^{Val}$ that had an altered 3′-CCA end revealed a depression of accuracy during the decoding of the next but one codon downstream (O'Connor et al., 1993). Obviously, a disturbance of the interaction of the tRNA with the ribosomal E site provoked an error increase in the selection process at the A site. This is precisely the effect that has been inferred from the reciprocal coupling of the A and E sites and has been demonstrated *in vitro* (Geigenmüller and Nierhaus, 1990; see above).

4. Is There More Than One State of the E Site?

Wintermeyer and co-workers have studied the translocation reaction with fast kinetic methods. They measured the fluorescent sig-

nals from dyes that were attached to deacyl-tRNA^{Phe} or AcPhe-tRNA^{Phe} and followed the time-resolved change of the fluorescent signal during the translocation of tRNAs from the P to the E site and from the A to the P site (Robertson et al., 1986). They also measured the kinetically resolved fluorescence energy transfer of dyes attached to the anticodon loops of the tRNAs during the translocation reaction (Paulsen and Wintermeyer, 1986). The change of the fluorescence signal could be described by three exponentials. The fast step had a rate between 1 s^{-1} and 5 s^{-1}, the intermediate step a rate between 0.1 s^{-1} and 0.3 s^{-1} and the slow phase occurred with a rate between 0.01 s^{-1} and 0.02 s^{-1}. The fast step was assigned to the simultaneous movements of the two tRNAs from A and P sites to P and E sites. The intermediate kinetic step was taken to represent a rearrangement of the E-site bound tRNA and the slow step was not assigned. During translocation, the distance of the two anticodon loops did not change significantly, being 23 ± 6 Å before and 25 ± 6 Å after (Paulsen and Wintermeyer, 1986). Therefore, the anticodon of the E-site bound tRNA should be in contact with the mRNA. In the course of the following rearrangement the distance between the anticodon loops increased to 34 ± 8 Å. The tRNA is supposed to dissociate during or after this process. Thus, the kinetics monitored during translocation of a tRNA from the P to the E site indicated two states of the E-site bound tRNA that the authors called E′ and E (Robertson et al., 1986). In E′, the first state reached after translocation, the anticodon is still in contact with the mRNA, and the mutual arrangement of the tRNAs is probably the same as before translocation. Thereafter, the codon-anticodon base pairs are disrupted during the subsequent rearrangement, and the tRNA reaches a position, that the authors call the E site; from this site the tRNA easily dissociates from the ribosome.

Such a rearrangement could not be observed under the experimental conditions of Nierhaus and colleagues. Analysis of PRE and POST complexes by neutron scattering revealed that the mutual arrangement of the two tRNAs does not change after translocation (Nierhaus et al., 1998). Probably, the kinetic intermediate state of Wintermeyer and colleagues (their so-called E′ state) is identical to the POST state of Nierhaus and colleagues. With this assumption, the different findings of the two groups concerning stability, codon-anticodon interaction, and the mutual arrangement of the P- and E-site located tRNAs in the POST state can be resolved.

Does the rearrangement of the E-site bound tRNA take place within an elongation cycle? A comparison of the rate constants of this rearrangement, 0.1 s^{-1} to 0.3 s^{-1}, with the rate of poly(Phe) synthesis under identical conditions, 5 s^{-1} (Robertson et al., 1986; Robertson and Wintermeyer, 1987), indicates that such a rearrangement with the reported rates is too slow to occur during one elongation cycle. The rate of the rearrangement is reminiscent of the rate reported for the dissociation of the E-site bound tRNA (see above), which was also one order of magnitude slower than a complete round of an elongation cycle. It follows that the ternary complex encounters a POST ribosome with occupied P and E sites and continuous codon-anticodon interactions in both sites, also in the experimental system of Wintermeyer and colleagues, as described by the allosteric three site model. The labile equilibrium state of the E site that was observed by Wintermeyer and colleagues (we term it the E2 site in the following, according to a suggestion by Valery Lim, personal communication) might represent an intermediate state of the tRNA, as it exists on the way out of the ribosome, that occurs as a short-lived intermediate during A-site occupation according to the allosteric three-site model. Different cross-linking patterns related to the presence or absence of codon-anticodon in-

teraction under conditions similar to those of the Wintermeyer group (Wower et al., 1995) provide evidence for two different locations of a tRNA reflecting the E and E2 positions. The E2 site is probably related to the position of the third tRNA found in an experiment where three deacylated tRNAs were bound to programmed ribosomes (Agrawal et al., 1996).

In summary, what we call the E site differs in three features from the E site observed by the Wintermeyer group: stable tRNA binding, codon-anticodon interaction at this site, and a mutual arrangement of the tRNAs at the P and E sites that is more or less identical to the arrangement in the pretranslocational state. These discrepancies concerning the features of the E site may be explained by the assumption that, after translocation, the ribosome is shifted back toward its PRE-state conformation as a result of the conventional buffer conditions and the ribosome preparation used by the Wintermeyer group. The attainment of a stable POST state is prevented, and instead a state is established that possibly represents a short-lived intermediate during the A-site occupation, viz., the state after the decoding process and before tight binding at the A site. Such a shift would negligibly affect the P-site bound tRNA with respect to the puromycin reaction. In this view the tRNA position at the E site, which is characterized by a stable binding, is different from the tRNA position E2, in which the tRNA easily falls off the ribosome. What we call the E site is obviously identical to the E′ site of Robertson et al. (1986), as both groups agree that codon-anticodon interaction is maintained at that site. The major difference is that in our case the features of the E site are stably realized, whereas those of the E′ site are not under the conditions used by Wintermeyer and colleagues. Recently, the stable E site and the labile E2 position could be directly visualized by cryo-EM using the polyamine system and the conventional system, respectively (Table 1). The E site provides a well-defined "envelope" covering the whole tRNA as does the P site. The mutual arrangement of the tRNAs in the P and E sites is very similar to that observed in the PRE state (Agrawal et al., 1998). In contrast, the tRNA in the E2 position seems to have only loose contacts with the ribosome and clings with its inner bend to L1 protein. This position was erroneously assigned as the E site in Agrawal et al. (1996) and Stark et al. (1997).

III. GENERAL TOPOGRAPHY OF THE TRNA BINDING SITES

Along with the functional characterization of the different ribosomal tRNA binding sites, the questions have been posed as to where these sites may reside within the ribosomal complex and which components of the ribosome may contribute to each site. Ribosomal components neighboring the tRNA in each site have been identified mainly by cross-linking and chemical protection analysis (summarized in Section III.A). The results in combination with other biochemical constraints have been used for modeling the tRNAs within ribosomal models (Sections III.B.1 and B.2). Recently, newer developments in electron microscopy and neutron scattering allowed for the first time direct determinations of tRNA positions in functional ribosomal complexes (Section III.B.3).

A. Defining the Ribosomal Components of Binding-Site Neighborhood

The most powerful tool for determining the ribosomal components that comprise the neighborhoods of the RNA ligands in defined functional states has been the cross-linking approach, which has been used exhaustively (for reviews see Wower and Zimmerman, 1991; Bogdanov et al., 1993; Brimacombe et al., 1993; Brimacombe, 1995). A whole

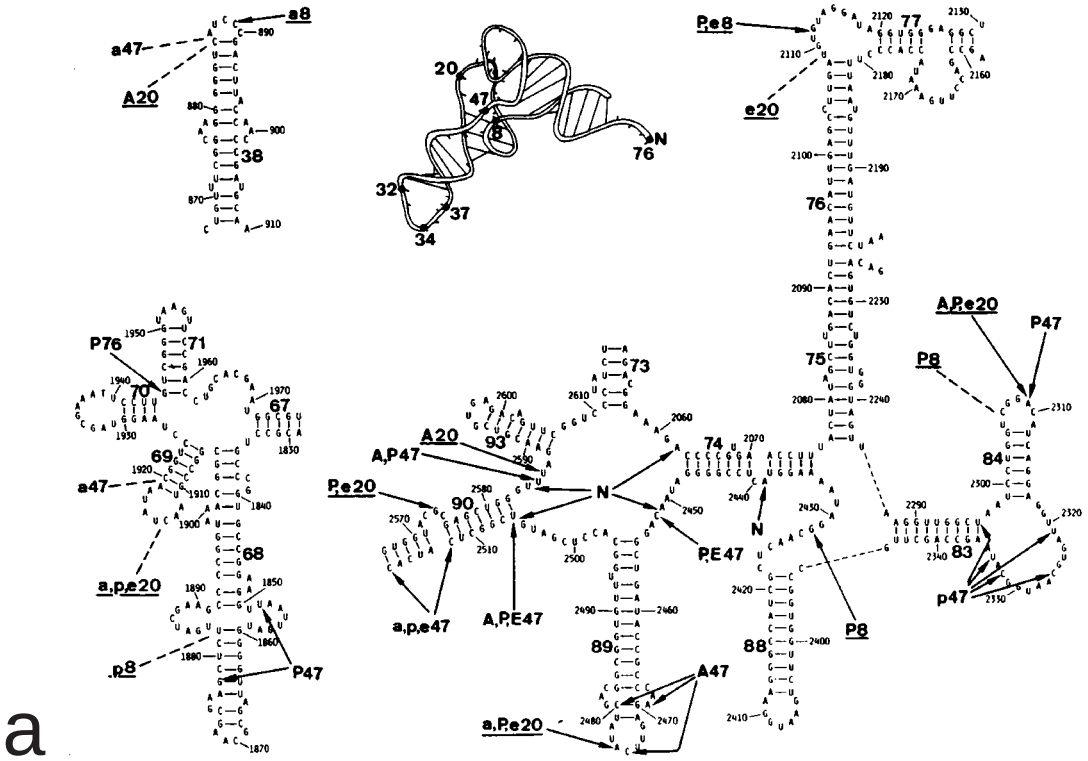

a

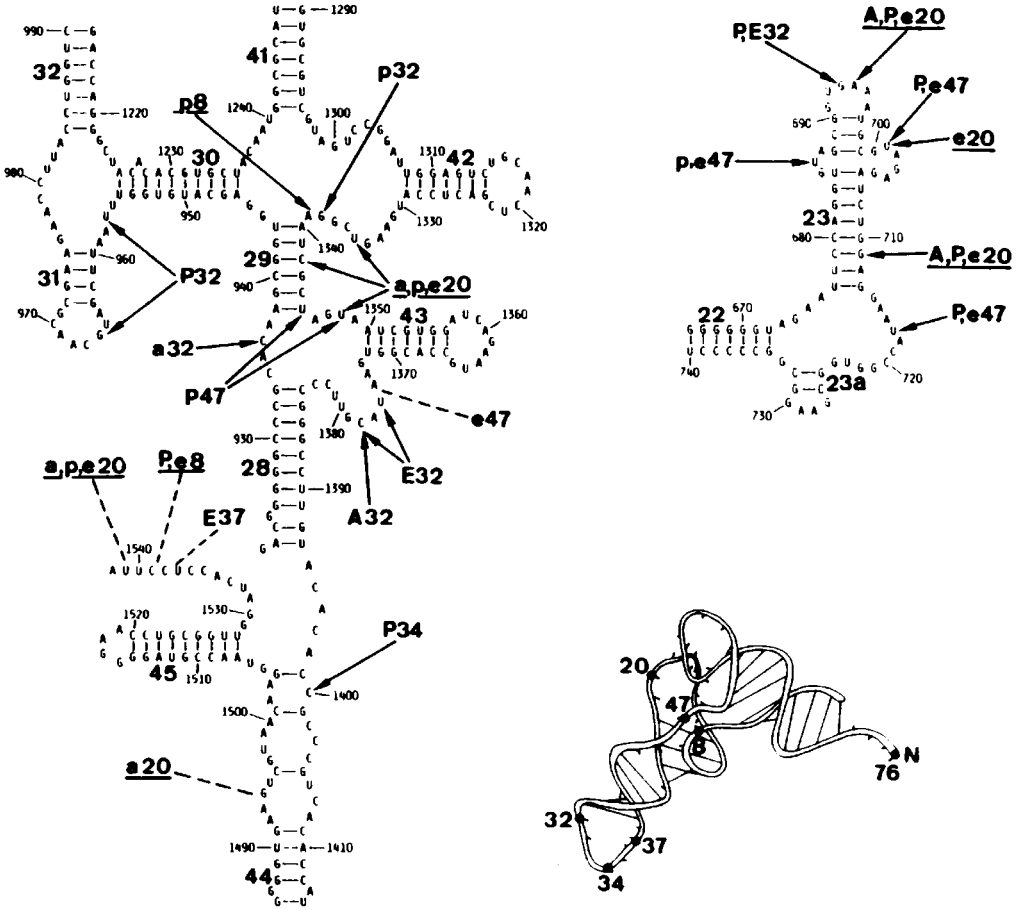

b

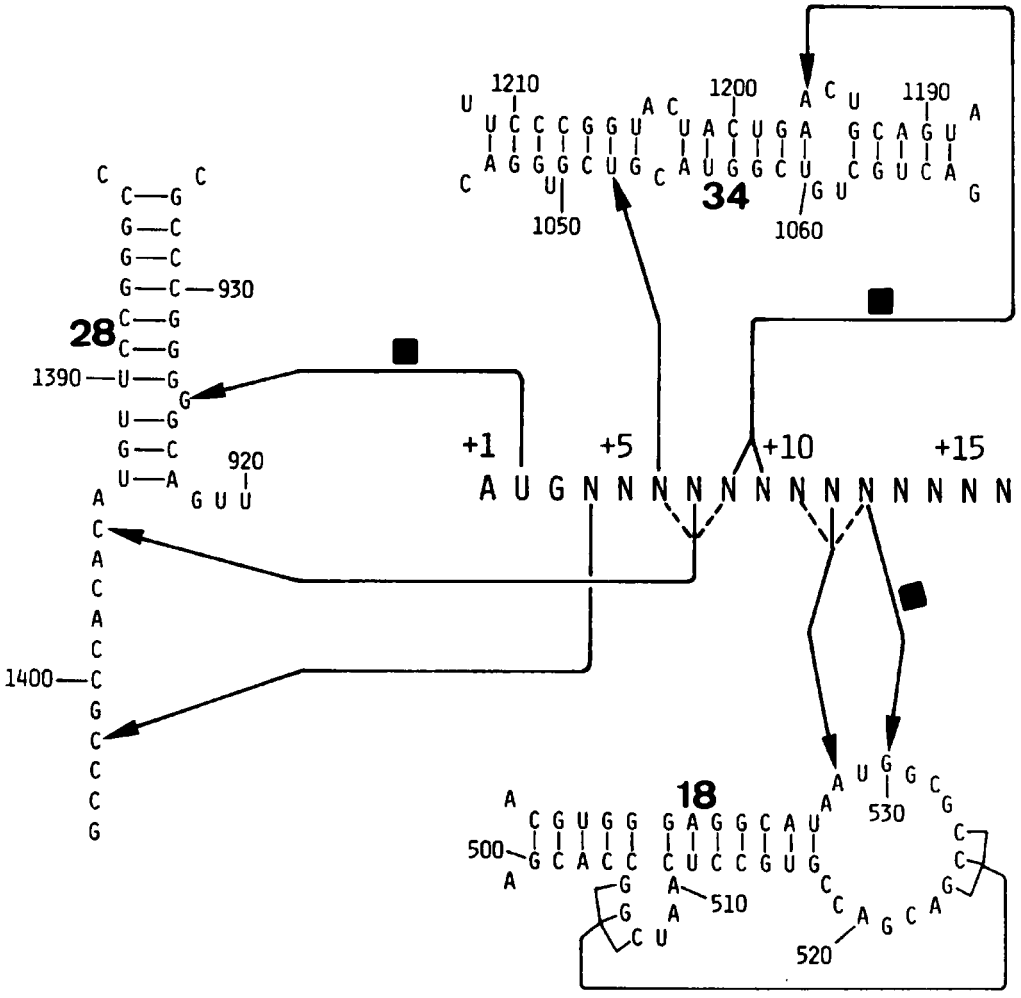

C

FIGURE 2. Microenvironment of RNA ligands on the ribosome as determined by cross-linking. **a, b**, Locations of cross-link sites from tRNAs on the 23S rRNA (a) and on the 16S rRNA (b). The sketch of a tRNA molecule indicates the positions from which cross-linking data are available (N denotes the aminoacyl residue). Cross-links are specified with a letter A, P, or E according to the binding site at which the tRNA is located (capital letters stand for major cross-links, small letters for minor cross-links and those not always seen) and a number that indicates the corresponding nucleotide position in the tRNA. **c**, Locations of cross-link sites from the mRNA on the 16S rRNA. In the center a generalized mRNA sequence (AUGNNN …) is shown. The arrows indicate the corresponding cross-link sites on the mRNA and on the 16S rRNA. Helices of the 23S and 16S rRNA are numbered according to Leffers et al. (1987) and Brimacombe (1991), respectively. (Reproduced with permission from Rinke-Appel et al., 1995, and Sergiev et al., 1997.)

network of neighborhoods could be established, as summarized in Figures 2 and 3. The cross-links of the rRNA ligands to the ribosomal RNAs are resolved at the nucleotide level (Figure 2). In contrast, in the case of protein cross-links, only the identity of the ribosomal protein is known but not the exact site of interaction (Figure 3).

Native tRNA may be directly cross-linked by far-UV irradiation (~254 nm). Nevertheless, this application is disadvantageous in that it induces damage to the ribosomal RNA and may therefore produce

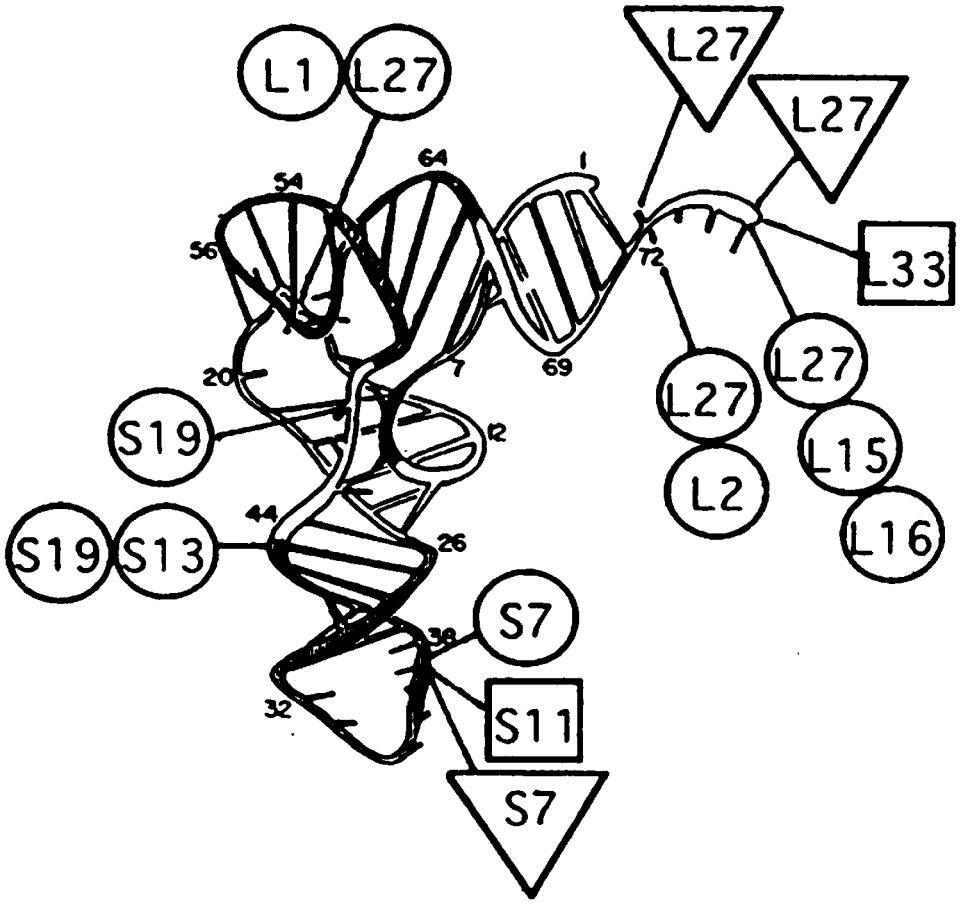

FIGURE 3. Microenvironment of tRNAs at the ribosome as determined by cross-linking. Cross-links from defined nucleotide positions in the tRNA to ribosomal proteins are shown. Proteins were differentially cross-linked depending on the location of the tRNA (A site, (triangles); P site, (circles); E site (squares). (Reproduced with permission from Wower et al., 1994.)

artifacts. Hence, it is preferable to use tRNA derivatives that can be photoactivated with near-UV light (300 to 360 nm) without damage to rRNA. Essentially two types of cross-linking studies have been performed to establish the above-mentioned network. The first method uses naturally occurring modified bases in the tRNA or the tRNA termini for the attachment of photoreactive reagents. Consequently, the cross-linking distance can be varied by the choice of appropriate cross-linking reagents (typically in the range from 8 to 15 Å). An alternative approach uses recombinant RNA techniques, which entail the random or site-directed incorporation of photoreactive nucleotide residues directly into the RNA structure (for reviews see Wower et al., 1994). Cross-links from the first method are less well defined than those obtained by the second method, but the number of cross-linking partners is higher. The second approach specifically establishes close neighborhoods since the cross-links are short ranged (2 to 4 Å). Thus, the two methods complement each other and are ideally suited to be combined in a molecular modeling process.

Figure 2 summarizes the available data concerning cross-linking between riboso-

mal RNA and the functional RNA ligands, tRNAs and mRNA. Data from chemical protection studies ("footprints") are highly correlated with the cross-linking results (Moazed and Noller, 1989a and 1990; for further discussion see Section IV and Brimacombe, 1995).

The equivalent information concerning cross-links to ribosomal proteins is depicted in Figure 3, except that here only cross-links from the tRNA in either binding site are considered (Wower et al., 1994). We note that a cross-link to the same protein does not necessarily mean that the same region of this protein is cross-linked. Because a ribosomal protein (molecular mass in the range of about 5 kDa to 30 kDa; S1 with a molecular mass of 61 kDa is exceptional) might be rather extended, the information provided by the protein cross-links is more important for establishing the general location of the tRNA binding site, rather than for allowing fine-tuned modeling as has been performed on the basis of the RNA cross-links (e.g., Brimacombe, 1995). However, cross-links to ribosomal proteins can also be refined to the amino acid level (e.g., Urlaub et al., 1995). Thus, amino acids neighboring the tRNAs in their binding sites will likely be characterized in the near future.

B. Models of tRNA Arrangement within the Ribosome

1. Models of the Ribosome

An essential prerequisite for revealing the spatial topography of the tRNA binding sites is a reliable and detailed knowledge about the structural framework, that is, the architecture of the ribosomal complex. Our current knowledge about the shape of the complex as well as the three-dimensional distribution of the different protein and RNA components has resulted essentially from studies applying electron microscopy (EM) and small angle scattering (SAS). Further refinement of the models was achieved by incorporating microtopographical data obtained by cross-linking and footprinting experiments. The resulting combined models display the structure in part already in molecular detail, although the reliability of the models has not yet reached that level of resolution. Thus, the incorporation of further experimental data may give rise to partial remodeling.

The basic structural features of the ribosomal subunits were revealed by visual inspection of negatively stained specimens using electron microscopy in the late seventies (see, e.g., Boublik et al., 1982; Oakes et al., 1986; Stöffler and Stöffler, 1986; Vasiliev et al., 1983). Accordingly, the 30S subunit appeared as a bipartite entity. The unequal-sized segments, assigned as head and body, are connected via a cylindrical element, called the neck. A characteristic extension, called either the platform or the lobe, projects from one side of the body almost parallel to the main axis of the subunit. As a result, a cleft is formed, bordered on either side by the platform extension and the neck element. In contrast, the 50S subunit appeared as a compact entity that is characterized by three cylindrical protuberances arranged along one side of the complex: the L7/12 stalk, the central protuberance, and the L1 protuberance. In the 70S ribosome the subunits are arranged in a way that the platform of the 30S subunit resides in close proximity to the L1 protuberance of the 50S subunit.

Two major drawbacks of the early EM studies limited the reliability and the resolution of the resulting models, that is, (1) the harsh conditions of specimen preparation, including extreme pH milieu as well as final air drying, and (2) the visual evaluation of the resulting electron micrographs. Both limitations were overcome, at least to some extent, by the introduction of cryo-EM and image reconstruction techniques, which, respectively, allow investigation of the ribosomal particles in an aqueous surrounding, that is,

in a hydrated state, and enable a statistical analysis of the electron micrographs (Frank, 1996). The improved methodology has been applied to a variety of ribosomal particles from different organisms (Frank et al., 1990). In 1991 Frank and co-workers presented the first cryoelectron microscopic reconstruction of the 70S ribosome from *E. coli* (Frank et al., 1991). The resulting model had a resolution of about 40 Å and attributed a rather spherical shape to the 70S ribosomal complex. Details of the envelope resembled the known features of the ribosomal subunits and thus allowed a tentative separation of the 70S volume into the putative 30S and 50S moieties. The striking feature of the model was a large cavity localized between the subunits and appears ideally suited to accommodate the ribosome-bound tRNA molecules.

In the latest refinements a resolution level of 20 to 30 Å was achieved. Two competing models of that quality, proposed by J. Frank and by M. v. Heel, are currently discussed (Frank et al., 1995a/b; Stark et al., 1995). Besides differences in a number of details, the major discrepancy resides in the structural organisation of the model volume. Frank's reconstruction (Plate 1a*) confirms the conventional view of the ribosome being essentially a compact entity. In contrast, v. Heel's model (Plate 1b) suggests a sponge-like organization of the ribosomal particle characterized by numerous internal solvent cavities.

Independent information about the architecture of the 70S ribosome and its isolated subunits was provided by small angle-scattering studies, essentially X-ray and neutron-scattering experiments (e.g., Crichton et al., 1977; Stuhrmann et al., 1977, 1978; Svergun et al., 1994a,b,c, 1997a,b). First of all, the scattering data allow a fairly direct validation of various discrepant models. Theoretical scattering curves corresponding to the different models can be calculated unequivocally. The deviation between the two calculated and the experimental curves quantifies directly the discrepancy among the two suggested models, as well as the discrepancy between either model and the solution structure of the ribosomal particle represented by the experimental curves. For the competing 70S models deduced from electron cryomicroscopy a validation of this kind was performed with respect to neutron solution scattering data (Svergun et al., 1997a). It turned out that neither of the two models agreed with the experimental scattering data in a comprehensive way. However, of the two, Frank's conventional compact representation fitted the data significantly better than v. Heel's sponge-like model, indicating that the former provides a better description of the solution structure of the 70S ribosome. As a control, a modified form of v. Heel's model containing matter in all internal solvent cavities was also evaluated. The theoretical scattering of the modified model met the experimental values as well as and in some cases even better than Frank's suggestion, indicating (1) that the sponge-like character of v. Heel's model was in fact decisive for the deviation of the theoretical scattering curves and (2) that the overall proportions of that model describe the solution structure of the 70S ribosome quite properly, in tendency even better than does Frank's model.

Besides the validation of models derived from other studies, neutron and X-ray SAS data allow independent model building (Stuhrmann et al., 1977, 1978; Svergun et al., 1994a,b; Svergun et al., 1997b). For the 50S subunit as well as for the 70S complex, models were deduced with respective resolutions of 40 Å and 35 Å (Svergun et al., 1994b; Svergun et al., 1997b). As one may expect from the direct validation of the two EM models, the solution scattering structure of the 70S complex (Plate 1c) was found to confirm the solid-body character of Frank's model, but it resembled v. Heel's shape with respect to its proportions.

* Plate 1 appears following page 122.

However, the major contribution of model building from solution scattering is in providing the internal protein-RNA distribution, which is difficult to deduce from electron microscopy. For the 70S ribosome, the particle volume could be divided into four phases representing the respective protein and RNA compartments of each subunit (Svergun et al., 1997b). Following the scattering analysis the total volume of the 70S complex was determined to be 4.0×10^6 Å^3, of which 2.4×10^6 Å^3 was attributed to the RNA moieties. Comparing these data to the model volumes of Frank's and Stark's EM-reconstructions of 3.9×10^6 Å^3 and 3.0×10^6 Å^3, respectively, one may rationalize that the differences of the models are, at least to some extent, caused by a higher threshold chosen in v. Heel's reconstruction, resulting in the representation of the dense regions of the particle essentially composed of rRNA. Similar discrepancies of EM models for the 50S subunit could previously be resolved in this way (Svergun et al., 1994b).

A further refinement of the shape models discussed so far resulted from the localization of the different ribosomal proteins achieved by immunoelectron microscopy (IEM) and small angle neutron scattering (SANS), respectively (Stöffler-Meilicke and Stöffler, 1990; Capel et al., 1987; May et al., 1992). Within the 30S subunit all proteins could be localized, and in most cases IEM and SANS provided consistent results. The protein positions were then used as reference points within the ribosomal shape in order to incorporate further microtopographical data obtained from crosslinking and footprinting experiments. In this way, RNA segments could be included, and, finally, rather comprehensive models for the 30S moiety—approaching in certain parts even molecular resolution—were constructed (Brimacombe et al., 1988; Stern et al., 1988; Malhotra and Harvey, 1994; Hubbard and Hearst, 1991). However, some problems arose in regions where IEM and SANS provided inconsistent protein positions, as in the cases of S12, S16, S19, and S20. Furthermore, a significant range of discretion remains for positioning the microtopographical evidence when the RNA is modeled with respect to the protein mass centers (discussed in Brimacombe, 1995). For that reason an alternative approach was used to refine the shape models by means of the cross linking and foot-printing data. This approach makes use of the recently achieved resolution level of the EM models in the range of 20 to 30 Å, which is compatible to the dimensions of the RNA double helix diameter (about 20 Å). Thus, the details of the model envelope suggest the position and orientation of helical segments of the ribosomal RNA. Combining these pieces of information with a number of highly resolved internal RNA crosslinks, a 16S rRNA model within the 30S moiety of the 70S complex was constructed (Stark et al., 1995; Brimacombe, 1995). In a second modeling step, the protein positions resulting from IEM and SANS were introduced and evaluated with respect to the location of the protected or cross-linked RNA segments. For most of the proteins, the data coincide rather well. In fact, in the cases of S19 and S20 the IEM positions were confirmed, whereas for S12 and S16 the positions provided by SANS fitted the 16S rRNA model much better (Brimacombe, 1995).

Unfortunately, the data on the spatial arrangement of the protein and RNA components within the 50S subunit are not nearly as complete as for the 30S subunit. Nevertheless, the growing wealth of information (May et al., 1992; Stöffler-Meilicke and Stöffler, 1990; Noller, 1991) have allowed first model building attempts (Walleczeck et al., 1988; Mitchell et al., 1990).

The shape of the ribosomal particle suggested from most of the experimental evidence, taken together, converges and allows refine-

ment to near-molecular resolution for the 30S moiety via incorporation of microtopographical data.

2. Molecular Modeling

The data from numerous biochemical studies (see Section III.A.) have been used to model tRNAs in the ribosome in combination with additional information from EM, neutron scattering, ribosomal models, and stereochemical constraints. At least for the tRNAs bound to A and P sites in the PRE state, there are severe restrictions for the relative tRNA arrangement. It is generally accepted that tRNAs in both the A and P sites simultaneously undergo codon-anticodon interactions with adjacent codons of the mRNA. On the other hand, the CCA ends of both tRNAs must to be neighboring to allow peptidyltransfer from the P to the A site. Thus, both tips of the L-shaped tRNA molecule must be in close proximity to the corresponding tips of the second tRNA.

Stereochemical considerations allow to discriminate two principal—and mutually exclusive—configurations of the two neighboring tRNAs in the elongating ribosome. In the first, the D-loop of the A-site bound tRNA faces the T-loop of the P-site bound tRNA with an enclosed angle between the two tRNA planes of about 90° (originally proposed by Sundaralingam et al., 1975; therefore, called the S configuration). In the R configuration (proposed by Rich, 1974) the situation is reversed in that the T loop of the A-site tRNA faces the D-loop of the tRNA in the P site, with an enclosed angle of about 100° (Lim and Venclovas, 1992). The R configuration has been favored on the basis of stereochemical arguments (Lim et al., 1992; Lim, 1997) premised on the crystal structure of free tRNAs (Kim et al., 1972, 1974; Robertus et al., 1974), but the S configuration may also be adopted, assuming that ribosome-bound tRNAs deviate slightly from their crystal structure. Evidence is available for conformational changes of the tRNA after binding (Möller et al., 1979; Dabrowski et al., 1995; Rodnina et al., 1995). Both configurations are depicted schematically in Figure 4, including the possible arrangements within the ribosome. It is obvious that the two configurations differ drastically in many biochemical aspects, for example, contacts of tRNAs with either subunit, tRNA elbows pointing either toward the 30S head (S) or the bridge region (R), and the relative position of the mRNA.

Besides stereochemistry, three further topographical constraints have been used for the arrangement in the ribosome as shown in Figure 4.

1. Codon-anticodon interaction takes place in the neck region of 30S subunit within the cleft formed by the platform, body, and head as revealed by IEM (Gornicki et al., 1984; Olson et al., 1988; Podkowinski and Gornicki, 1989).
2. The peptidyltransferase center of the ribosome is believed to be located at the base of the central protuberance, where antibiotics interfering with the peptidyltransferase activity have been localized by IEM and affinity labeling (e.g., Olson et al., 1982, 1985; Cooperman et al., 1990). This view is supported by the results of cross-linking studies (Wower et al., 1989).
3. The ternary complex aminoacyl-tRNA·EF-Tu·GTP, which brings the tRNA to the A site, enters the ribosome from the L7/L12 side (Girshovich et al., 1986), and thus the A site is assumed to be nearer to L7/L12 and the P-site bound tRNA to be more inside the ribosome. The crystal structure of the ternary complex has been solved recently (Nissen et al., 1995; Plate 2a*), allowing further evaluation of both models.

* Plate 2a appears following page 122.

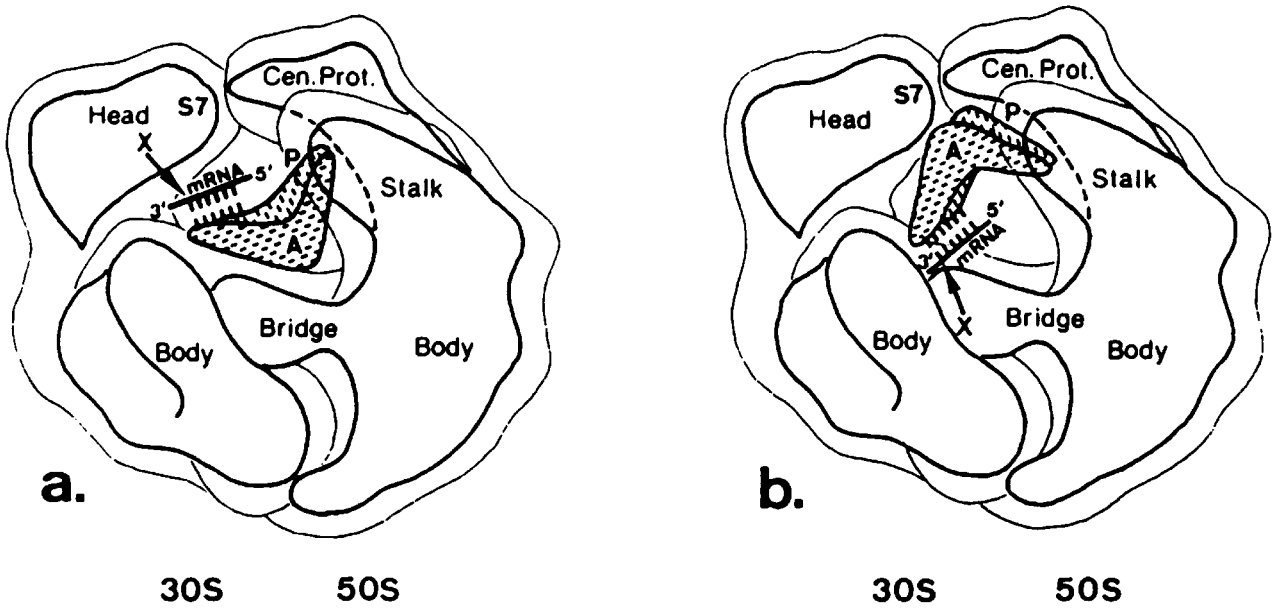

FIGURE 4. R and S configurations of A- and P-site bound tRNAs. **a**, R configuration; **b**, S configuration; tRNAs are depicted by the hatched symbols (the A-site bound tRNA in the front, the P-site bound in the back). The sketch of the 70S ribosome follows Frank et al. (1991); the 30S subunit is on the left, the 50S subunit on the right; their structural features are indicated (Cen. Prot., central protuberance; S7, position of the S7 epitope according to IEM. (Reproduced from Lim et al., 1992, with permission of Oxford University Press).

The crystal structure revealed that EF-Tu binds the tRNA mainly at its 3′ and 5′ ends and at its T stem.

Consequently, a simple way of guiding the tRNA to the A site would result in a situation where the D side of the tRNA in the ternary complex faces the P-site tRNA (S configuration; see Plate 2c). However, two further points must be considered: (1) the footprint on 16S rRNA is almost identical for tRNA in the ternary complex and for A-site bound tRNA (Moazed and Noller, 1990), and in both cases the tRNA is protected by the ribosome in a similar manner (Dabrowski et al., 1995). (2) Domains III to V of EF-G have a striking morphological similarity to the aminoacyl-tRNA within the ternary complex (Nissen et al., 1995), thus representing the first demonstrated instance of protein mimicry of an RNA molecule. Even the path of negative charges arising from the phosphate groups at the T side of the anticodon stem is mimicked by domain IV of EF-G (Liljas et al., 1995; Plate 2b). We assume that the tRNA-mimic of EF-G interacts with the decoding center after translocation, thus preventing a back-translocation, as long the factor lowers the activation energy barrier between the PRE and POST states (Nierhaus, 1996). If this assumption is correct, the location of the path of negative charges strongly argues in favor of the view that the tRNA contacts the decoding center at the anticodon arm from the T side. This would suggest that the T side of a tRNA is its side of contacts both with EF-Tu at the acceptor arm (T stem and loop plus acceptor stem) and with the ribosomal decoding center at the anticodon arm.

The seemingly divergent observations can be reconciled as follows: the A-site occupation is separated into at least two steps. The first step comprises the interaction of the anticodon arm with the decoding center at the A site. It is an interaction of the ternary complex with the low-affinity A site and represents the decoding reaction *sensu strictu*. At this stage EF-Tu does not interact with the ribosome and thus does not cause a steric conflict. When the decoding reaction has been completed successfully, the second step can be initiated, comprising two events that are probably coupled: the EF-Tu-dependent GTPase is triggered, leading to a release of this factor, and the A site is converted into its high-affinity state, in which the ribosome can also interact at those tRNA regions that were previously occupied by the elongation factor. This high-affinity binding is a prerequisite for the subsequent peptidyltransfer.

Arranging tRNAs within the ribosome by modeling approaches depends on the availability of reliable, highly resolved ribosomal models. Detailed knowledge about the distribution of the components is needed to fully exploit the information about neighborhoods. The available models (compare Section III.B.1) have been used for proposing structural models of the tRNA arrangement within the ribosome based on biochemical data about neighborhoods (Section III.A). Most of the newer models show an S-type configuration (e.g., Wower et al., 1989, 1993b; Figure 5a; and Noller et al., 1990; Figure 5b), whereas older models tended to assume an R-type configuration (e.g., Lake, 1977; Spirin, 1983).

Previously, in a combinatorial approach taking into consideration the stereochemistry and biochemical data the R configuration had been favored (see discussion in Lim et al., 1992). More recently, crosslinks from the mRNA to 16S rRNA nucleotides probably located in the 30S body (Rinke-Appel et al., 1994) were taken to favor the S configuration, and a model for the tRNA arrangement was proposed (Figure 5c; see discussion in Brimacombe, 1995). In fact, the tRNA locations in the three different models depicted in Figure 5 are quite similar and differ only in minor details. On the other hand, V. Lim put forward stereochemical arguments for an

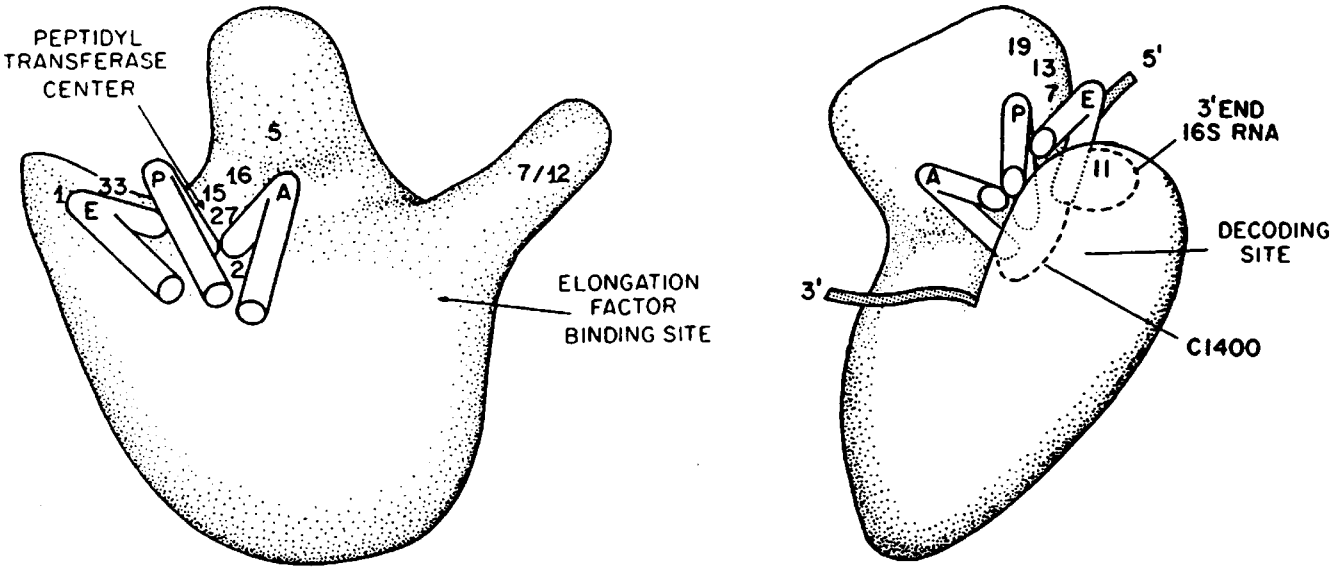

FIGURE 5. Models for the tRNA arrangement on the ribosome. tRNA positions in A, P, and E sites viewed from the interface sides of the 50S and 30S subunit (a, c) or within the 70S complex (b). **a,** According to Wower et al. (1993b): Numbers indicate locations of epitopes of ribosomal proteins derived from IEM. (Reproduced with permission from Wower et al., 1993b.) **b,** According to Noller et al. (1990): Hatched area shows the approximate site of interaction of the ternary complex. (Reproduced with permission from Noller et al., 1990. Copyright 1990 American Society for Microbiology, ASM Press.) **c,** According to Brimacombe (1995). (Reproduced with permission from Brimacombe, 1995.) Silhouettes of the subunits follow (a, b) Oakes et al. (1986) and (c) Frank et al. (1991).

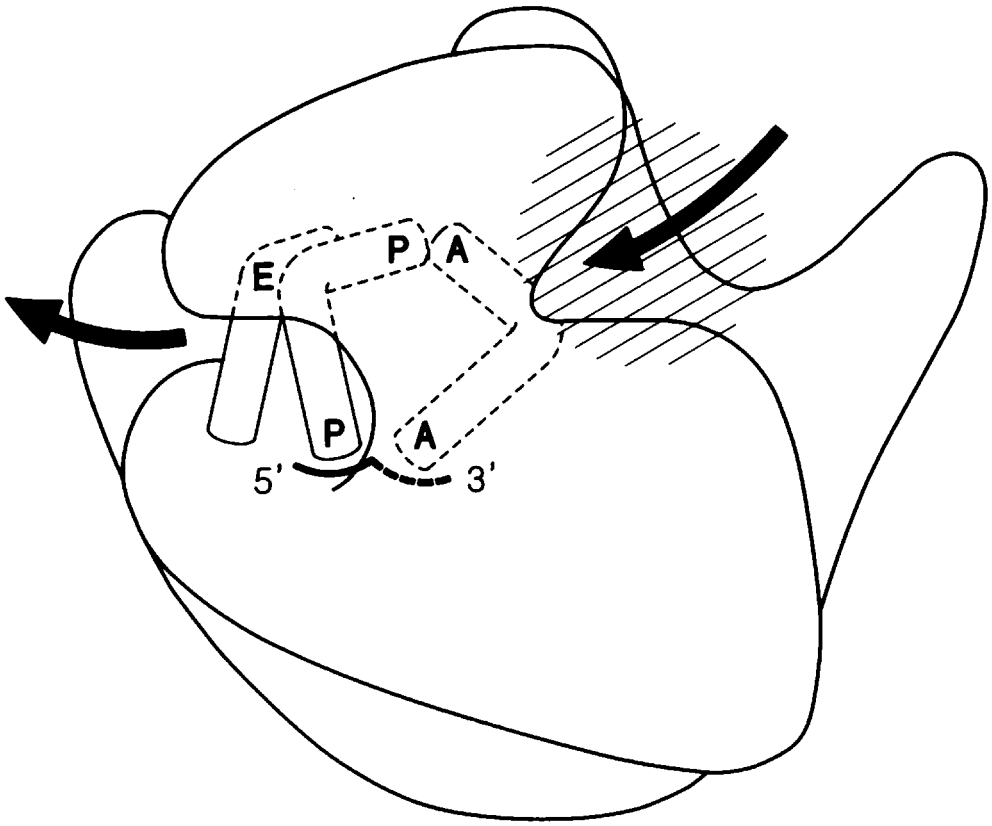

FIGURE 5B

R configuration of the codon-anticodon duplex on the ribosome (Lim, 1997).

Recently, the tRNA nucleotides protected by either subunit have been analyzed using iodine cleavage at phosphorothioated residues. Most of the tRNA is shielded by the 50S subunit, and only the anticodon loop and part of the stem is protected by the 30S subunit (M. A. Schäfer and K. H. Nierhaus, manuscript in preparation). This finding is unexpected from the models shown in Figure 5, because in these the tRNA runs in parallel with the 30S subunit, with mainly the acceptor stem pointing toward the 50S subunit. The protection results could be explained more easily if tRNAs were arranged in the R configuration (Figure 4) assuming that the bridge region belongs to the 50S subunit. In that case, the tRNA would mainly contact the 50S subunit. Indeed, the four-phase model derived from neutron scattering (Section III.B.1, Plate 1c) assigns this region to be part of the 50S subunit.

3. Direct Determinations

Because modeling of tRNAs in defined sites based on biochemical constraints depends on detailed knowledge about the location of ribosomal components, it would be particularly advantageous to have direct information on the tRNA location independent of the distribution of ribosomal components. Only recent developments in physical methods such as electron microscopy and neutron scattering have made it possible to acquire this kind of direct information. In the following we summarize some of the main

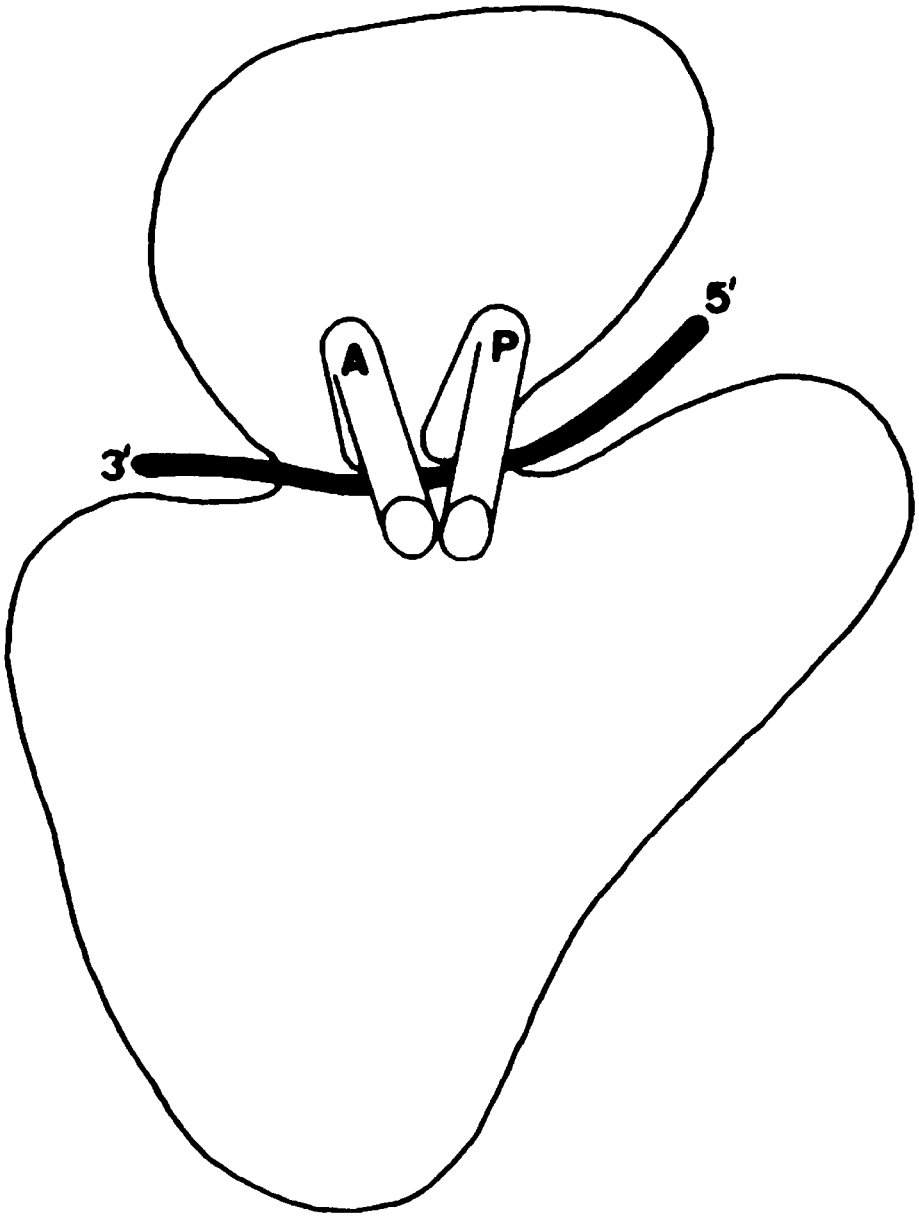

FIGURE 5C

progress in these technologies and discuss their first contributions to the question of localizing tRNA binding sites.

As already discussed (see Section III.B.1), new developments in electron microscopy have resulted in major improvements both in measuring native states of the biological specimen (samples in vitreous ice; low electron doses necessary) and in the level of resolution. Using techniques of three-dimensional image reconstruction, electron microscopy-derived ribosome models have achieved a resolution of about 20 to 30 Å (Frank et al., 1995a/b; Stark et al., 1995). In principle, this level of resolution allows the visualization of tRNA molecules that have an overall size

of about 75 Å (Kim et al., 1974). To achieve this direct visualization, the three-dimensional density map of ribosomes carrying tRNA molecules is compared with the density distribution of empty ribosomes, and the difference density is calculated in each point. This difference mass can be attributed mainly to the ligands (tRNAs and mRNA) but may also be partially caused by structural changes of the ribosome after functional complex formation, leaving some uncertainties in the interpretation. This type of analysis has been used recently to localize tRNAs in poly(U) programmed ribosomes saturated with deacylated $tRNA^{Phe}$ (Agrawal et al., 1996) by comparison with a model obtained from vacant 70S ribosomes (Frank et al., 1995a/b). Three tRNA molecules could be fitted to the difference density found in the interface cavity and were assigned to the ribosomal binding sites A, P, and E (see Section II) according to biochemical constraints. In this model (herein referred to as the EM-Frank-model; Plate 3a-c*) the A- and P-site bound tRNAs enclose an angle of about 160° with their anticodons and CCA ends in close proximity. Further processing revealed that the enclosed angle between A and P site tRNAs is probably smaller, in the order of 110° (J. Frank and S. Harvey, personal communication). The anticodon ends are located at the neck region of the small subunit, but on the L7/L12 side of the channel within this neck (Frank et al., 1995; Lata et al., 1996), rather than on the platform side where codon-anticodon interaction has been placed in previous studies (Gornicki et al., 1984; Olson et al., 1988; Podkowinski and Gornicki, 1989). The CCA ends point toward the entrance of a tunnel, located at the bottom of the interface canyon, which has been proposed to provide the exit path for the nascent peptide chain (Frank et al., 1995b). The E-site assigned tRNA is found in a position dislocated from the two other tRNAs, with its anticodon distant from A- and P-sites anticodons, thus excluding the possibility of codon-anticodon interaction from this site. We note, however, that the complex containing three deacylated tRNAs does not represent a native state during ribosomal function (see Sections II and IV). Nevertheless, the so-called E site in this model may be related to the E2 site (Section II.C.4.) in a complex that is suggested to be a short-lived intermediate during the transition to the PRE state containing three tRNAs (an aminoacyl-tRNA (A site), a peptidyl-tRNA (P site), and a deacylated tRNA (E site, exiting the ribosome in the course of the A-site occupation). Therefore, the third tRNA seen by Agrawal et al. (1996) probably does not represent the E-site location in a POST elongation complex, when the A site is free.

More recently, functional ribosomal complexes have been examined representing the two main elongation states, the PRE and the POST states. An assignment of the two tRNA molecules present in both states would in principle allow description of the movement of a tRNA through the ribosomal binding sites A, P, and E and would thus be a milestone in our structural understanding of ribosomal function. Similar studies have been performed by two groups independently (Stark et al., 1997; Frank and Nierhaus, unpublished), although differently prepared complexes were analyzed. In the first one, PRE complexes prepared *in vitro* have been compared with native disomes taken as representing the POST state. In the respective difference masses relative to a vacant ribosome model (Stark et al., 1995) or relative to the second elongation state, two tRNAs could be fitted in either state (Stark et al., 1997), interpreted as A- and P-sites or P- and E-sites bound tRNAs, respectively (Plate 3d-f; herein referred to as the EM-van-Heel-model). The P site is found to be identical in PRE and POST, lying directly above the bridge that connects the sub-

* Plate 3 appears following page 122.

units. The A site is located at the L7/L12 side of the P-site tRNA with an angle between the tRNAs of about 50°, and with the elbows of both tRNAs pointing toward the 30S head (S configuration). The anticodons of both tRNAs meet in the 30S neck region, and the CCA ends are directed toward the 50S subunit. The E-site tRNA is situated such that the anticodon tip lies above the side lobe of the 30S subunit, resulting in a distance between the anticodon loops of the P- and E-site tRNAs of about 54 Å. The elbow of the E-site bound tRNA is proximal to the L1 protuberance, with the CCA end near that of the P-site bound tRNA.

The data evaluation in the second EM study is yet not completed (J. Frank and K. H. Nierhaus, unpublished). Here a PRE/POST pair was examined that had been prepared *in vitro* starting from a single biochemical preparation (for preparation details see Wadzack et al., 1997). At the present state of data analysis some conclusions can already be drawn. The differences masses were found to be very similar in PRE and POST, with a shift of about only 10 Å toward the L1 protuberance from PRE to POST. Furthermore, it follows that no tRNA is lost during translocation and that translocation is not accompanied by a gross conformational change of the tRNA arrangements relative to each other. A detailed discussion is presented elsewhere.

Besides EM, the second physical technique allowing the direct assessment of tRNA positions in the functioning ribosome is neutron scattering. Its application in biological structure research relies on the different scattering behavior of hydrogen when compared with the other main elements found in biological samples, including deuterium, the heavier isotope of hydrogen. This difference provides the basis for specifically labelling defined components by isotopic exchange of hydrogen vs. deuterium. Neutron scattering has been applied successfully in the last decades to localize ribosomal proteins either in the 30S (Capel et al., 1987) or in the 50S subunit (May et al., 1992), although different procedures for sample preparation had to be used for the two subunits (for discussion see Nierhaus et al., 1983). In contrast, mapping of RNA ligands in the 70S ribosome has not been possible because of the sheer size of the 70S ribosome and the low contrast of RNA ligands in the neutron beam. RNA molecules contain only about 33% hydrogen (when compared with about 50% of all atoms in proteins), and hence the experimental variability of the contrast by hydrogen-deuterium exchange is limited. Therefore, the question of RNA ligand location could only be addressed by neutron scattering after the development of an improved method, the proton-spin contrast variation (Stuhrmann, 1989, 1991; Knop et al., 1991). This technique exploits the dependence of hydrogen scattering length on the nuclear spin orientation relative to the spin of the incoming polarized neutrons. By an alignment of proton and neutron spins, the signal of small protonated components embedded in a deuterated matrix can be selectively amplified by more than one order of magnitude, and thus small ligands such as the RNA ligands in the functioning ribosome become detectable (Stuhrmann et al., 1995; Wadzack et al., 1997; Jünemann et al., 1997). Only limited information like the radius of gyration or the distances between mass centers of the protonated ligand and the deuterated ribosome can be determined directly without using any knowledge about the ribosomal or the ligand structure. More sophisticated interpretations, for example, the localization of the ligand complex or the determination of internal arrangements, are most easily extracted from the scattering data by referring to a model for the ribosome and for the ligand complex.

The method of proton-spin contrast variation has been applied to determine the position, orientation, and mutual arrangement

of the two tRNAs simultaneously present on the elongating ribosome in the PRE and the POST states. As a model for the ribosome the EM model of J. Frank and co-workers was used (Plate 1a; Frank et al., 1995a/b). The mass center of the RNA ligand complex was found to be located in the interface cavity near the neck of the 30S subunit. After translocation from the PRE to the POST state the mass center is shifted by 12 ± 4 Å toward the head of the 30S subunit and slightly toward the platform side of 30S (Wadzack et al., 1997). For the data processing a simple eight-spheres model describing the two L-shaped tRNA molecules was introduced. This model allowed us to extract the orientation and the mutual arrangement of the two tRNAs within the elongating ribosome (Nierhaus et al., 1998). The deduced model for the tRNA arrangement is depicted in Plate 3g-i. As in the EM studies described above, the two tRNA molecules are indistinguishable, and thus the assignment of the tRNAs to the ribosomal binding sites relies solely on considerations based on information from other studies. The tRNA molecule painted green is proposed to reside in the A site in the PRE state (Plate 3g,h) and in the P site in the POST state (Plate 3i). Correspondingly, the red tRNA should be in the P or E site, respectively. The translocational movement necessary to proceed from the PRE to the POST state is rather small when compared with the huge displacements inferred from the EM studies. It can be described mainly by a rotational movement by about 18°, shifting the mass center by only about 12 Å toward the head of the 30S subunit. The mutual arrangement of the two tRNAs remains constant after translocation: the anticodon tips and the CCA ends of both tRNAs are in close proximity in either state, with an angle between the tRNA planes of about 110° ± 10°. However, using another 70S model for data processing an angle of ~50° is found before and after translocation (Nierhaus et al., 1995). It follows that the angle between the tRNA planes is model dependent and thus cannot be extracted from the neutron scattering data at this stage of processing, whereas the model-invariant finding of a constant mutual arrangement of the tRNAs before and after translocation can be considered as solid information.

A further interesting aspect of the model inferred from neutron scattering is that, unexpectedly, the P-site bound tRNA is located at strikingly different positions in the PRE and the POST states (compare the red tRNA in Plate 3h with the green in Plate 3i), suggesting that the "P site" is not a topographically consistent site, despite reflecting the operational criterion of puromycin reactivity. This might be taken as a first indication that the three operationally defined sites might not correspond to three topographically fixed entities (further pieces of evidence are discussed in Section IV).

Taken together, three detailed proposals for the tRNA arrangement in the functioning ribosome derived from direct physical methods (two EM studies and one neutron scattering study) are presently available. All three proposals show consensus on the assignment of three tRNA binding sites on the *E. coli* ribosome (A, P, and E sites), in agreement with functional studies (see Section II). Also, the general location of the tRNAs within the interface cavity, with the anticodons pointing toward the 30S neck region and the CCA ends directed to the base of the 50S central protuberance, is consistent among them. Nevertheless, the models are conflicting in a number of important details as discussed below.

tRNA configuration. An important point of controversy is whether the tRNAs are bound to the ribosome in the R or the S configuration (see Section III.B.2; Lim et al., 1992, 1997). The neutron scattering analysis cannot distinguish between R and S configuration. Both EM studies favor an S configuration. Nevertheless, the difference map, on which the EM-Frank-model is based, leaves

some freedom for interpretation, also allowing an R-type configuration (V. Lim, personal communication).

Angle between tRNA planes. The angle between the two tRNAs in the PRE state is about 50° in the EM model of v. Heel and co-workers (Stark et al., 1997) and also in a model derived from a recent reconstructon by the Frank group (J. Frank, personal communication).

Site of codon-anticodon interaction. In all models codon-anticodon interaction takes place in the neck region of the 30S subunit. The neutron scattering model and the EM-van-Heel-model propose codon-anticodon interaction at the platform side of the neck but significantly closer to the head of the 30S subunit in the neutron scattering model. The site of the anticodons is shifted to the side of 30S facing the L7/L12 stalk in the Frank model.

Translocational movement and E-site properties. A major discrepancy between the different models is the proposed translocational movement and the resulting arrangement of the E-site bound tRNA. In the neutron-scattering model the mutual arrangement of the two tRNAs is maintained after translocation, whereas both EM models assume a disjointed E site, although the amount of displacement varies. In the van-Heel-model mainly the anticodon region of E-site bound tRNA is shifted by 54 Å from the anticodon loop of the P-site bound tRNA. The translocational movement is described by a relatively small rotation combined with a lateral translation toward the L1 protuberance. The E site in the Frank model is attained by a rotation of 145° from the corresponding P site combined with an shift by approximately 20 Å. This results in a situation where the anticodon, as well as the CCA end of the E-site bound tRNA, is distant from the respective ends of the tRNA in the P site. Although the two EM models are incompatible with respect to the position of the E-site bound tRNA, both exclude codon-anticodon interaction at this site. In contrast, the neutron-scattering model implies that both tRNAs are shifted *en bloc* and thus easily maintain simultaneous codon-anticodon interaction with the mRNA, in agreement with considerable biochemical evidence (Section II. C.2).

There are a number of possible reasons for the discrepancies described above.

1. The nature of the biological samples is strikingly different in all three studies. The EM-Frank-model was based on one preparation of poly(U)-programmed ribosomes saturated with deacyl-tRNA^{Phe}. This resulted in ribosomes with three tRNAs bound simultaneously. Consequently, the discussion of PRE to POST transition is necessarily rather speculative and relies on the assumption that the state examined portrays native binding sites that are assumed to be topographically constant after translocation. The other two studies compared two sets of complexes assumed to represent either the PRE or the POST state. In the second EM study (van-Heel-model) the PRE state was prepared *in vitro* by succesive filling of P and A sites and was compared with native polysomes (*in vivo* disomes), which were treated with EF-G *in vitro* in order to maximize the fraction of POST-state complexes. The buffer conditions used (6 m*M* Mg^{2+}, no polyamines) are known to inactivate ribosomes (Rheinberger and Nierhaus, 1987). For the neutron scattering study the PRE state was prepared rather similarly (despite different buffer conditions and different tRNAs used), but the POST state was achieved by incubating half of the prepared PRE state with EF-G to establish the POST state (PRE and POST states were verified by the puromycin reaction). Thus, in this preparation both elongation states were

derived from the same biochemical preparation.

2. The methods used for structure determination are different. This is obvious when comparing EM with neutron-scattering techniques, but even the two EM studies themselves are different with respect to data collection, contrast transfer function correction, and reconstruction approach, which may cause significant discrepancies (Zhu et al., 1997). We note, however, that all methods discussed here allow the sample to be measured in a frozen state in aqueous environment. This is a particular advantage, as samples can be kept in a defined native state during measurements.
3. At the present level of resolution neither technique allows direct visualization of the individual tRNAs, thus leaving room for interpretation. The difference mass obtained by subtracting vacant ribosomes from the functional complex (or by subtracting functional complexes from each other) is not well enough defined that the tRNA molecules can be fitted unambiguously. Peaks in the difference map may be due to the mRNA, which is not considered in the present models (including that derived by neutron scattering), or to conformational changes of the ribosome after tRNA binding or translocation, and may thus be misleading for a straightforward interpretation of tRNA location. On the other hand, the neutron scattering analysis strongly depends on the precision with which biochemical and physical parameters have been determined (compare Wadzack et al., 1997) and on the quality of the models used for data processing.

The conflicting features ascribed to the ribosomal tRNA binding sites in the different models argue for the need for further studies. Currently, an EM analysis of an authentic PRE/POST pair derived from one preparation and biochemically very similar to the PRE/POST pair analyzed by neutron scattering using the polyamine system is underway (J. Frank and K. H. Nierhaus, unpublished. The results so far obtained can be summarized as follows: (i) The difference masses allow an unequivocal assignment of the tRNA positions in the various sites. (ii) An E site is observed at a position not seen before, that provides a mold for the overall shape of a deacylated tRNA. Codon-anticodon interaction is possible at this site, and the mutual arrangement of the tRNAs is not significantly changed before and after translocation. This E site position provides all the features ascribed to the E site by the allosteric three-site model. (iii) Under conventional buffer conditions an E2 site is observed (erroneously described as "E site" by Agrawal et al., 1996, and Stark et al., 1997, see Section II.C.4). At the E2 position the tRNA clings with its inner bend to the mushroom-like structure of the L1 protuberance probably in a labile fashion. The E and the E2 positions are obviously mutually exclusive, that is to say, a tRNA is found either in the E site or in the E2 position. It follows that the E2 site marks a transient tRNA position on the way out of the ribosome after the tRNA has left the E site. The E2 position has all the features ascribed by Wintermeyer and co-workers to the "E site" using conventional buffer conditions, i.e., easy drop off, labile binding and the absence of codon-anticodon interaction (Wintermeyer et al., 1990). Obviously, the authentic E site escaped their attention, because the unfavorable conventional buffer system and washed ribosomes were used (see Section C.1). A model of the functional complexes including the tRNAs at atomic resolution must await crystallographic analysis. Progress in this direction has been made (e.g., Eisenstein et al., 1991; Franceschi et al., 1993), but probably it will be at least

several more years before such data become available.

IV. MICROTOPOGRAPHY OF tRNA BINDING SITES AND EVOLUTION OF THE BINDING SITE CONCEPT

On the basis of tRNA binding studies three sites, namely, the A, P, and E sites, could be distinguished, which show different properties with respect to the various tRNA species, viz., deacyl-, aminoacyl-, or peptidyl-tRNA (Sections II.A, II.C). Functional studies revealed an intimate interplay between the sites as for instance described in the allosteric three-site model (Section II.B). The tRNA binding sites were thought to be characterized by distinct topographies within the ribosomal complex. During protein synthesis the tRNAs occupy these sites in the order A→P→E. Accordingly, the translocation movement from one binding site to another was rationalized as an unidirectional diffusion process mediated by the affinities for the different tRNA species (e.g., Spirin, 1985).

Hardesty and co-workers provided the first experimental evidence suggesting that the view of the tRNA binding sites as being spatially fixed entities may be an oversimplified description (Hardesty et al., 1986). Using the fluorescence energy transfer method they could demonstrate that the position of a P-site bound deacyl-tRNA is significantly different from that of a P-site bound peptidyl-tRNA analogue (AcPhe-tRNA). The distances to the ribosomal proteins L11 and S21 were used as reference values in this study. The non-equivalent position of the two tRNA species was unexpected at that time, but it could be discussed as being compatible with the generally accepted view of an operationally defined P site. A further study suggesting an E site (stable binding) and an E2 site (labile binding) has already been discussed in Section II.C.3 and 4.

In order to characterize tRNA binding within the structural framework of the ribosome, comprehensive RNA-footprinting studies were performed. The investigation of the micro-environment of the tRNAs during elongation yielded detailed insights about the binding mode of these ligands and allowed mechanistic models for the tRNA's translocation movement to be developed.

In the following, we summarize footprinting experiments on the ribosomal RNAs that led to the hybrid state concept for tRNA binding (Section IV.A., the hybrid-site model). Then, a complementary study focusing on contact patterns on the tRNAs, which defined the dynamic domain concept (Section IV.B., the α-ε model), is outlined.

A. The Hybrid-Site Model

Most of the footprinting experiments on the ribosomal RNAs were performed by Noller and co-workers (summarized in Moazed and Noller, 1989b). As tRNAs bind specifically to the A, P, and E sites, the rRNAs receive different protections against modification. Thus, the various tRNA binding states can be correlated with characteristic protection patterns on the 16S and 23S rRNA. An AcPhe-tRNA bound to the P site defined the "P-site pattern", while binding of a ternary complex Phe-tRNA·EF-Tu·GTP to the A site after prefilling the P site with a deacylated tRNA resulted in the "A-site pattern". The "E-site pattern" — not so well defined in the poly(U)-dependent system used — was derived from the binding of deacylated tRNA requiring an intact 3′-CCA terminus.

The major conclusion was derived from a comparison of the protection patterns before and after the peptidyltransferase reaction. In the case of a P-site bound AcPhe-tRNA, the protection pattern on the 23S rRNA changed from a pattern characteristic for the P site to

a pattern characteristic for the E site after peptide-bond formation with puromycin, whereas the pattern on the 16S rRNA remained unaltered. The selective change of the 23S rRNA pattern was taken as indication that the acceptor end of the tRNA already reaches the E-site position after peptidyltransfer, and before translocation. This tRNA location was called a hybrid binding state, abbreviated P/E state; the binding state before peptidyltransfer was termed the P/P state. (In this notation, the letter before the slash refers to the 16S rRNA pattern and that after the slash to the pattern on the 23S rRNA, indicating the localization of the bound tRNA on the 30S and on the 50S subunit, respectively.)

In a related experiment, a ternary complex was added to ribosomes carrying an AcPhe-tRNA^{Phe} at the P site. Peptide bond formation is expected to occur spontaneously, resulting in a complex with an AcPhe-Phe-tRNA bound at the A site and a deacylated tRNA at the P site. The footprinting analysis of the final complex revealed an A plus P pattern on the 16S rRNA and a P plus E pattern on the 23S rRNA. The same pattern was obtained when an AcPhe-tRNA^{Phe} was present at the A site along with a deacylated tRNA at the P site; here no peptide bond formation could follow the occupation of the A site. Extending the concept of the hybrid binding state, the authors described the peptidyl-tRNA analogue as being bound in the A/P state and the deacylated tRNA in the P/E state. After translocation of the tRNAs, P/P and E patterns were observed, respectively. Since no characteristic 16S rRNA pattern could be defined, the E site was concluded to be located essentially on the 50S subunit in accordance to earlier studies (Kirillov et al., 1983; Gnirke and Nierhaus, 1986).

The derived hybrid-site model for the elongation cycle is shown in Figure 6. Following that scheme, each tRNA moves through the ribosome in an alternating fashion, that is, with one extremity (the acceptor end or the anticodon tip) fixed while the other is moving. On the 30S subunit the scenario follows the classical scheme, that is, a movement is seen only during translocation (Section II.B). On the 50S subunit the corresponding shift precedes translocation. The acceptor ends already move during the peptidyltransferase reaction, while the anticodon is fixed on the 30S subunit.

The hybrid-site model describes three different PRE elongation complexes with a tRNA at the A site, namely, a tRNA in the A/T, A/A or A/P state (the classical scheme comprises only two states, related to A/T and A/A; T referring to the specific protection pattern of the ternary complex on the 23S rRNA, which do not overlap with the A-site pattern induced by the tRNA alone, that is, after the release of EF-Tu). Furthermore, due to the alternating nature of the movement, the tRNAs are always in a binding contact with the ribosome. Thus, translocation attains the character of a guided replacement rather than a random, diffusion-like movement as in the classic models. Because high precision in translocation is essential for maintaining the reading frame, this step should be carefully controlled by the ribosome.

In an alternative presentation of the hybrid-site model (the "ratchet model"), the shift of the 23S rRNA protection pattern accompanying the peptidyltransfer is attributed to a rearrangement of the two subunits, that is, a relative movement of the 30S with respect to the 50S subunit that reverses during translocation. This alternative view postulates a conformational change of the ribosome as being possibly the major event during translocation and, if correct, would provide the first hint as to why ribosomes require the universal two-subunit structure.

Note that according to the hybrid-site model the peptidyl residue is in the P-site region after peptidyltransfer (peptidyl-tRNA in the A/P state), but it does not react with puro-

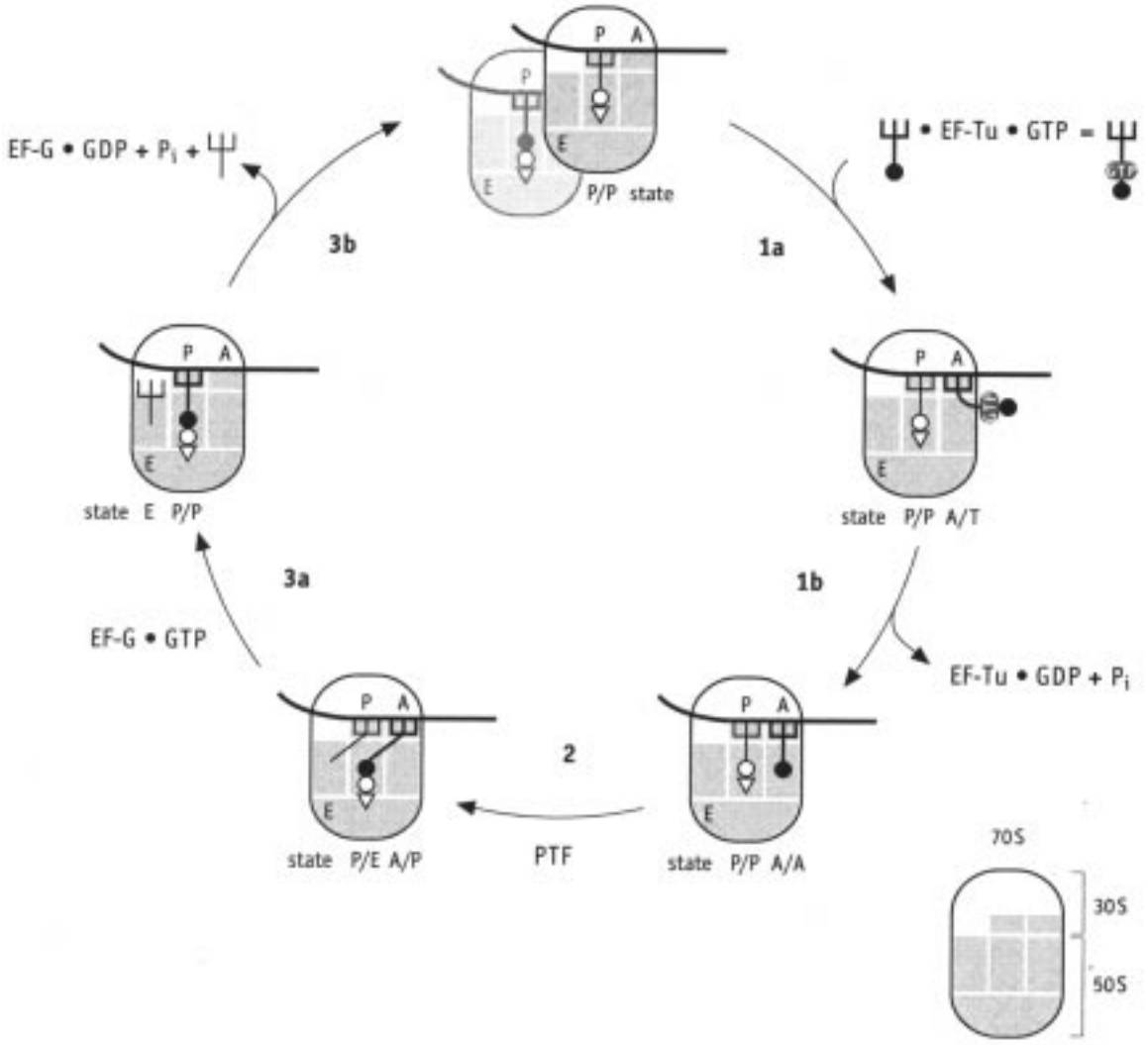

FIGURE 6. The hybrid-site model for the elongation cycle. According to this model the tRNAs move through the ribosome in such a way that they change binding sites on the 30S and 50S subunit in an alternating fashion. tRNAs thereby pass through hybrid binding states, that is, states in which they are bound on the 30S and 50S subunits at different sites. 1, A-site occupation; 1a, selection of the cognate ternary complex aminoacyl-tRNA·EF-Tu·GTP (A/T binding state); 1b, fixation of the cognate aminoacyl-tRNA (A/A binding state) and release of EF-Tu·GDP. 2, Peptidyl-transfer (PTF); rearrangement of the acceptor ends of the A- and P-site bound tRNAs (switch from A/A and P/P to A/P and P/E binding states, respectively). 3, translocation; 3a, EF-G dependent switch of the tRNAs from A/P and P/E to P/P and E binding states, respectively; 3b, release of EF-G·GDP and of the E-site bound tRNA (for further explanations see text; adapted from Moazed and Noller, 1989b).

mycin. Consequently, two P-site positions on the 50S subunit must be distinguished in the framework of the model, one puromycin-reactive and one puromycin-non-reactive in contrast to the classic definition.

Furthermore, the hybrid-site model predicts that a posttranslocational elongation complex with a peptidyl-tRNA in the P site and a deacylated tRNA in the E site releases the latter after puromycin treatment (that is, the

P-site bound tRNA changes from the P/P to the P/E state, thus chasing the deacylated tRNA at the E site). However, this prediction could not be confirmed experimentally: when POST state ribosomes within native polysomes were subjected to a puromycin reaction, most of the E-site bound tRNA remained bound (Remme et al., 1989).

A closer inspection of the protection data reveals that the protection patterns on the 23S rRNA mainly reflect the position of the extreme acceptor end of the tRNA, as the protection of 16 out of 17 bases was dependent on the A-3′ or CA-3′ of the universal 3′-CCA tRNA terminus (Moazed and Noller, 1989a). The described tRNA movement preceding translocation should therefore be understood as a local displacement of the 3′-CCA ends rather than a relocation of large parts of the tRNA body. The same reasoning implies that the structural rearrangement suggested by the hybrid-site model is a local ribosomal event rather than a gross conformational change of the ribosomal complex. This view is in good agreement with the results of an X-ray small angle scattering study comparing PRE and POST elongation complexes, which revealed no significant shape differences between the two states (Svergun et al., 1997b).

A further limitation of the experimental data is seen in the fact that a huge range of Mg^{2+} concentrations, ranging from 5 to 25 m*M*, was applied in various experimental settings (Moazed and Noller, 1986, 1989a,b). It is well known that the binding properties and the interdependencies of the various sites are extremely sensitive to changes of the Mg^{2+} concentration (Rheinberger and Nierhaus, 1987). This sensitivity probably reflects an increasing distortion of the ribosome with increasing Mg^{2+} concentration, which may well affect a fine-structure analysis such as the chemical probing of the rRNA bases.

One of the major aspects of the hybrid-site model, namely, the continuous binding contact of the tRNAs to the ribosome, was confirmed and further extended by footprinting experiments on the tRNAs, which is outlined in the following section.

B. The α-ϵ Model

For examination of the contact patterns of ribosome-bound tRNAs, a recently introduced footprinting technique was applied (Schatz et al., 1991; Dabrowski et al., 1995, 1998). tRNA transcripts were prepared *in vitro* containing a few phosphorothioated nucleotides, A, G, U, or C, at random positions. For probing the transcribed tRNAs, iodine (I_2) was used to cleave the accessible thioated phosphodiester bridges with low efficiency. Due to the small size of the I_2 molecule, this method exclusively reveals those phosphates that are very closely protected, and thus are good candidates for an intimate contact to the ribosome.

The tRNA contact patterns were examined in PRE and POST elongation complexes carrying a deacylated $tRNA^{Phe}$ and an AcPhe-$tRNA^{Phe}$ at A and P sites and at P and E sites, respectively (Dabrowski et al., 1995, 1997). The two PRE complexes were made by (1) binding thioated AcPhe-$tRNA^{Phe}$ to the A site of poly(U)-programmed ribosomes carrying a native $tRNA^{Phe}$ in the P site, and (2) filling the P site with thioated $tRNA^{Phe}$ and binding native AcPhe-$tRNA^{Phe}$ to the A site. The corresponding POST complexes were made from the respective PRE complexes via EF-G-dependent translocation. The authenticity of the complexes was confirmed by the puromycin reactivity of the AcPhe-residue, that is, by making use of the operational definition of the ribosomal binding sites.

The footprinting analysis of the PRE complexes revealed strikingly different protection patterns of the A-site bound and

P-site bound tRNAs. About 60 positions covering the whole tRNA molecule (except for a small number of nucleotides at the 3′- and 5′-ends) could be monitored in either site, and 41 of these differed between the A-site and the P-site bound tRNAs (Dabrowski et al., 1995). The corresponding analysis of the POST complexes provided contact patterns for the P- and E-site bound tRNAs, which — unexpectedly — closely resembled those of the A- and P-site bound tRNAs of the PRE complexes, respectively. In a comparison of the patterns of the thioated AcPhe-tRNA^{Phe} at A and P sites, one finds that only 7 out of 63 positions differed in accessibility. In the case of the deacylated tRNA^{Phe} at P and E sites, only one out of 61 positions was identified as reacting significantly differently. Obviously, as a rule the nucleotides in contact with the ribosome hardly change during translocation.

The type of pattern observed on the AcPhe-tRNA^{Phe} at the A site before translocation and at the P site after translocation was termed α (α, because at the A site only α-like patterns are found). Correspondingly, the pattern revealed on the deacylated tRNA^{Phe} at the P site before translocation and at the E site after translocation was named ε (ε, because at the E site only ε-like patterns are found). Because close contact is necessary for protection against iodine cleavage, it was proposed that the α and ε patterns might reflect the ribosomal microenvironment of the tRNAs, that is, the binding sites or, more generally, the ribosomal components responsible for tRNA fixation. This interpretation seems to be justified by a recent study in which the contact pattern of a thioated tRNA bound to its cognate aminoacyl-tRNA synthetase was analyzed (Schatz et al., 1991). The crystal structure of that complex solved shortly afterwards confirmed that the contact pattern obtained from iodine cleavage is directly related to the pattern of molecular contacts between tRNA and the protein (Biou et al., 1994). Making use of this observation, the fact that the protection patterns of the ribosome-bound tRNAs, α and ε, remain unaltered, was taken as an indication that the two tRNAs do not change their ribosomal binding domains during translocation, in contrast to the classic understanding.

However, it is known that (1) the mRNA moves three nucleotides (one codon) through the ribosome in the course of translocation (e.g., Beyer et al., 1994, and references therein), and (2) the mass center of gravity of the two tRNAs combined moves by about 12 Å within the ribosome (Wadzack et al., 1997), in good agreement with the length of one codon. In addition, thermodynamic studies have shown that translocation is accompanied by a conformational change of the ribosomal complex (Schilling-Bartetzko et al., 1992b). In order to reconcile the experimental pieces of evidence mentioned previously, one has to assume that the conformational change results in a movement of the tRNAs in space, while their immediate molecular environment is kept unchanged. The simplest explanation is that a movable α-ε domain exists that is capable of binding two tRNAs at its α and ε regions, respectively (Dabrowski et al., 1998). The movable domain would display the α and ε sites at the A and P positions before translocation and at the P and E positions after. At the A site only α could appear and at the E site only ε, whereas at the P site α and ε could be alternatively present, depending on the functional state of the ribosome. In the following we retain the operational definitions of A, P, and E sites, and speak about α and ε as the *ribosomal tRNA binding domain* α-ε.

The concept of a dynamic tRNA binding domain provides a new understanding of the tRNA binding mode and results in a modified scheme for the elongation cycle presented in the α-ε model (Plate 4*). Besides the dynamic domain concept, another well-documented experimental fact was taken into account in the development of the α-ε model: when a programmed ribosome is saturated

with deacylated tRNA, the first tRNA occupies the P site and the second occupies the E site, thus establishing the POST state. With a large excess of tRNAs over ribosomes, a third tRNA can be bound to the A site, which is obviously in a low-affinity state (Rheinberger et al., 1981). Furthermore, the decoding process occurs in the POST state, with P and E sites occupied. Thus, a tRNA can interact with the A site when the ribosome is in the POST state, that is, when the α-ε domain is in the P-E position. This observation is rationalized by assuming a decoding center "δ" firmly installed at the A-site region of the 30S subunit. δ would be separate from the α-ε domain in the POST state but would overlap with α in the PRE state.

Following the scheme for the elongation cycle according to the α-ε model (Plate 4*) the occupation of the A-site region proceeds in the two steps, 1a and 1b. During the decoding process (step 1a) the ribosome is in the POST state, that is, the α-ε domain is in P-E position, thus fixing the peptidyl-tRNA in the P-site region by α and the deacylated tRNA in the E-site region by ε. The selection of the cognate ternary complex is accomplished via codon-anticodon interactions at the decoding center δ. The correct codon-anticodon interactions established by the cognate aminoacyl-tRNA trigger the shift of the α-ε domain from the P-E to the A-P position (step 1b). The α-ε domain releases the tRNAs in the P and E sites, in order to bind the ones in the A and P sites, respectively. As a result, the selected aminoacyl-tRNA is now tightly bound to α at the A-site region, the peptidyl-tRNA resides in the P-site region now fixed by ε, and the deacylated tRNA leaves the ribosome, possibly passing a location similar or equivalent to the E2 position (see Section II.C.4). In the following step the peptide chain is transferred to the aminoacyl residue of the A-site bound tRNA (peptidyltransferase reaction, step 2). During the third step (translocation reaction, step 3) the α-ε domain shifts back from the A-P to the P-E position, with the two tRNAs firmly bound by α and ε, respectively. This results in the relocation of the bound tRNAs from the A and P sites to the P and E sites and thus establishes the POST state, which is competent for the next decoding reaction (step 1a).

According to the α-ε model, the translocation of the tRNAs (step 3) results from a controlled movement of the domain α-ε to which the tRNAs remain firmly bound. Thus, translocation is described as a precisely controlled structural rearrangement as required for keeping the reading frame of the translation process. In the a-e model the critical step is not the translocation, as in previous models, but rather the reaction 1b of the A-site occupation, that is, the fixation of the cognate tRNA. The view that reaction 1b is characterized by a major rearrangement between the $(tRNA)_2$·mRNA complex and the ribosome is consistent with the observation that the occupation of the A site, rather than translocation, is the rate-limiting step of the elongation cycle (Schilling-Bartetzko et al., 1992b; Bilgin et al., 1988).

Furthermore, the concept of the α-ε domain can be easily reconciled with structural studies that have shown that the spatial localization of P-site bound tRNAs is not identical in different functional states of the ribosome (as outlined above in this section, cf. Hardesty et al., 1986, and in Section III.B.3., cf. Wadzack et al., 1997). Another study focused on the ribosomal neighborhood of a deacylated tRNA bound to P and E sites using a cross-linking approach (Bullard et al., 1995). Up to five 4-thiouridines were randomly incorporated in the tRNA under study and further modified by attaching a phenanthroline. These residues cleave nucleic acids in the presence of Cu^{2+} ions within a radius of about 20 Å. 118 cleavage sites were detected, and 85% of

* Plate 4 appears following page 122.

these were identical at P and E sites, in good agreement with the concept of a dynamic binding domain.

Note that all three features of the allosteric three-site model (Section II.B) are valid in the α-ε model as well, although they are extended or reinterpreted.

1. Three tRNA binding sites exist on the ribosome but are separately exposed only in the POST state (α and ε with high tRNA binding affinity, and δ with low affinity). In the PRE state, α and δ overlap, resulting in only two distinct high-affinity tRNA binding sites (α + δ and ε).
2. The reciprocal relationship of A and E sites appears as an immediate consequence of the dynamic domain concept for the tRNA-binding sites. When the α-ε domain is in the A-P position, the E site has no affinity for tRNAs. In the other case, when the α-ε domain is in the P-E position, the A site is of low affinity due to the decoding center δ.
3. Simultaneous codon-anticodon interactions of both tRNAs are maintained in the course of translocation, since their mutual arrangement and their arrangement relative to the mRNA do not change.

A further study using iodine footprinting focused on the protection patterns of tRNAs bound to 30S and 50S ribosomal subunits (M. A. Schäfer and K. H. Nierhaus, manuscript in preparation). It turned out that most of the nucleotides protected in the 70S complexes are also found to be inaccessible in the 50S complexes. Only the upper part of the anticodon stem loop appeared to be covered by the 30S subunit (positions 29 ± 1 to 41 ± 1 of the tRNA). Because the 30S and the 50S patterns, taken together, closely resemble the respective 70S patterns, the analysis suggests a partition of the latter into a 30S and a 50S moiety. As the 50S pattern covers most of the nucleotides on the tRNA's surface, the tRNA binding apparatus of the ribosome should reside mainly on the 50S subunit. A challenging task for future studies will be to identify the ribosomal components, comprising this domain. As the contact patterns of the tRNAs demonstrate contacts over the whole tRNA molecule, from the anticodon loop down to the acceptor stem, the ribosomal binding apparatus for the tRNAs must bridge both subunits. Of the six bridges that have been identified between the subunits, only one, bridge 2 in the authors' terminology, connects the decoding region of the 30S subunit with the peptidyltransferase region of the 50S subunit (Frank et al. 1995a; Lata et al., 1996; see Figure 7). This bridge is the most massive connection between the subunits and thus is the prime candidate for the α-ε domain. In agreement with the footprinting results the bridge region is mainly attributed to the 50S subunit (Section III.B.1). One component of this important structure seems to be the ribosomal protein L2 (G. Diedrich, M. A. Schäfer, R. Jünemann, and K. H. Nierhaus, manuscript in preparation). Other candidates were already suggested from cross-linking experiments outlined in Section III.A.

The protection pattern on the tRNA due to the 30S subunit comprises only the anticodon loop and a part of the corresponding stem. Consequently, the tRNA-induced protection patterns on the ribosomal 16S rRNA, discussed in Section IV.A, monitor the micro-environment of mainly the anticodon regions of a tRNA. Taking further into account that most of the 23S rRNA protections depend on the structure of the 3′-end of the tRNAs (Section IV.A), the footprinting data on the ribosomal RNAs appear to indicate essentially the location of the extremities of the bound tRNAs, namely, the anticodon and the acceptor ends. A rearrangement of the acceptor ends during the peptidyl

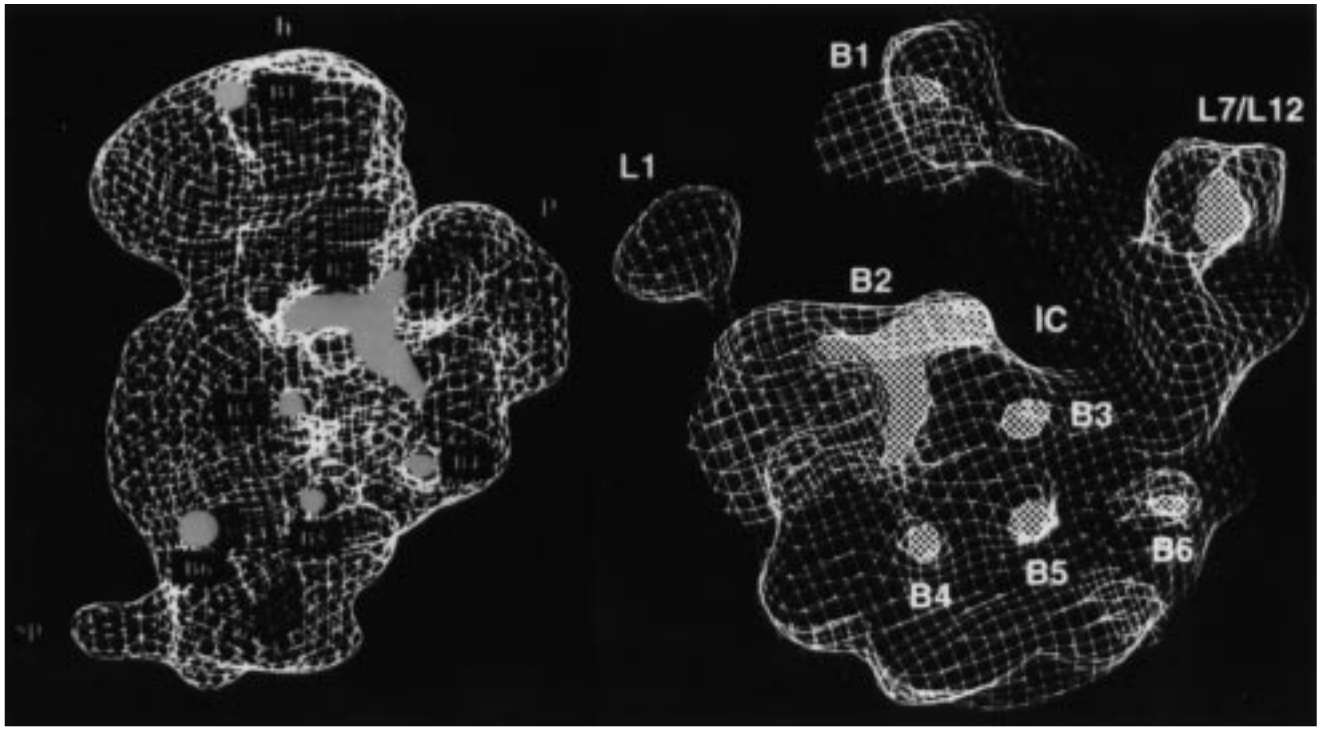

FIGURE 7. Intersubunit bridges (B1-B6) within the 70S ribosome shown from the interface sides of the 30S and 50S subunits (white contours). 30S (left): h, head; sp, spore; p; platform. 50S (right): L1, L1 protuberance; IC, interface canyon; L7/12, L7/12 stalk. (Reproduced with permission (left) from Lata et al., 1996. Copyright 1996 Academic Press Ltd., London, England, and (right) from Frank et al., 1995a. Copyright 1995 NRC Research Press, Ottawa, Canada.)

transfer, that is, before translocation, can be easily reconciled with the dynamic domain concept and is incorporated in the refined version of the α-ε model (Plate 4). The movement of the anticodon ends during translocation, indicated by the change of the protection patterns on the 16S rRNA, is in accord with the classical view of tRNA movement.

In the framework of the α-ε model, translocation is accompanied by the separation of α and δ, thus taking into account a change of the microenvironment around the anticodon ends, but keeping the molecular neighborhood of the majority of the tRNA molecules unchanged. Thus, the experimental results that provide the basis for the hybrid site model fit the dynamic α-ε-domain concept and are taken into account in the refined version of the α-ε model (Plate 4). However, the hybrid site model extrapolates from the rearrangement of the flexible 3′-CCA end toward a rearrangement of the whole tRNA molecule during peptidyl transfer resulting in the major discrepancy between this model and the α-ε model: the tRNAs are described to move in an alternating fashion in the hybrid-site model, whereas they move *in toto*, that is, on both subunits simultaneously, in the α-ε model.

Taken together, the two footprinting studies lead to the conclusion that the operationally defined tRNA binding sites do not correlate in a simple fashion with distinct structural entities on the ribosome. Translocation and A-site binding result mainly from structural rearrangements of the ribosomal complex in the course of the elongation cycle, which allow the different functional states to be established in a precisely controlled way. Therefore, appropriate models for the ribosomal tRNA binding sites must consider the dynamic nature of the elongation complex. The α-ε model introduced the concept of a dynamic tRNA binding domain that binds both tRNAs tightly at the A and P sites and carries the tRNAs to the P and E sites, respectively, during translocation. This concept makes it possible to reconcile most of the experimental data of structural and functional studies available to date and lays the foundation for a mechanistic scheme for the elongation cycle.

ACKNOWLEDGMENTS

We are grateful to Drs. Rajendra K. Agrawal, Joachim Frank, Pawel Penczek, and Adriana Verschoor for help and discussion.

REFERENCES

Agrawal, R. K., Penczek, P., Grassucci, R. A., Gabashvili, I.S., Heagle, A. B., Sriviastava, S., Burkhardt, N., Jünemann, R., Nierhaus, K. H., and Frank, J. 1998. Proc. 14th Int. Congr. Electron Microscopy 1998, in press.

Agrawal, R. K., Penczek, P., Grassucci, R. A., Li, Y., Leith, A., Nierhaus, K. H., and Frank, J. 1996. Direct visualization of A-, P-, and E-site transfer RNAs in the *Escherichia coli* ribosome. *Science* **271:** 1000–1002.

Bartetzko, A. and Nierhaus, K.H. 1988. Mg^{2+}/NH_4/ Polyamine system for polyuridine-dependent polyphenylalanine synthesis with near in vivo characteristics. *Meth. Enzymol.* **164:** 650–658.

Berchtold, H., Reshetnikova, L., Reiser, C.O., Schirmer, N.K., Sprinzl, M., and Hilgenfeld, R. 1993. Crystal structure of active elongation factor Tu reveals major domain arrangements. *Nature* **365:** 126–132.

Bilgin, N., Kirsebom, L.A., Ehrenberg, M., and Kurland, C.G. 1988.

Mutations in ribosomal L7/L12 perturb EF-G and EF-Tu functions. *Biochimie* **70:** 611–618.

Beyer, D., Skripkin, E., Wadzack, J., and Nierhaus, K.H. 1994. How the ribosome moves along the

mRNA during protein synthesis. *J. Biol. Chem.* **269:** 30713–30717.

Biou, V., Yaremchuk, A., Tukalo, M., and Cusack, S. 1994. The 2.9 Å crystal structure of *T. thermophilus* seryl-tRNA synthetase complexed with $tRNA^{Ser}$. *Science* **263:** 1404–1410.

Boublik, M., Robakis, N., Hellmann, W., and Wall, J. S. 1982. Electron microscopic study of eukaryotic 40S initiation complex in protein synthesis. *Eur. J. Cell. Biol.* **27:** 177–184.

Brimacombe, R. 1991. RNA-protein interactions in the *E. coli* ribosome. *Biochimie* **73:** 927–936.

Brimacombe, R. 1995. The structure of ribosomal RNA: A three-dimensional jigsaw puzzle. *Eur. J. Biochem*. **230:** 365–383.

Brimacombe, R., Atmadja, J., Stiege, W., and Schüler, D. 1988. A detailed model of the three-dimensional structure of *Escherichia coli* 16S ribosomal RNA *in situ* in the 30S subunit. *J. Mol. Biol.* **199:** 115–136.

Brimacombe, R., Döring, T., Greuer, B., Jünke, N., Mitchell, P., Müller, F., Osswald, M., Rinke-Appel, J., and Stade, K. 1993. Mapping the functional centre of the *Escherichia coli* ribosome. **In:** *The Translational Apparatus—Structure, Function, Regulation, Evolution.* pp. 433–444. Nierhaus, K. H., Franceschi, F., Subramanian, A. R., Erdmann, V. A., and Wittmann-Liebold, B., Eds., Plenum Publishing Cooperation, New York.

Brow, D. A. and Noller, H. F. 1983. Protection of ribosomal RNA from kethoxal in polyribosomes. Implication of specific sites in ribosome function. *J. Mol. Biol.* **163:** 27–46.

Bullard, J. M., van Waes, M. A., Bucklin, D. J., and Hill, W. E. 1995. Regions of 23S ribosomal RNA proximal to transfer RNA bound at the P and E sites. *J. Mol. Biol*. **252:** 572–582.

Capel, M. S., Engelman, D. M., Freeborn, B. R., Kjeldgaard, M., Langer, J. A., Ramakrishnan, V., Schindeler, D. G., Schneider, D. K., Schoenborn, B. P., Sillers, I.-Y., Yabuki, S., and Moore, P. B. 1987. A complete mapping of the proteins in the small ribosomal subunit of *Escherichia coli*. *Science* **238:** 1403–1406.

Chinali, G. and Parmeggiani, A. 1982. Differential modulation of the elongation-factor-G GTPase activity by tRNA bound to the ribosomal A-site or P-site. *Eur. J. Biochem.* **125:** 415–421.

Cooperman, B. S., Weitzmann, C. J., and Fernández, C. L. 1990. Antibiotic probes of *Escherichia coli* ribosomal peptidyltransferase. **In:** *The Ribosome: Structure, Function, and Evolution*. pp. 491–501. Hill, W. E., Dahlberg, A., Garrett, R. A., Moore, P. B., Schlessinger, D., and Warner, J. R., Eds. American Society for Microbiology, Washington, D.C.

Crichton, R. R., Engelman, D. M., Haas, J., Koch, M. H. J., Moore, P. B., Parfait, R., and Stuhrmann, H. B. 1977. Contrast variation study of specifically deuterated *Escherichia coli* ribosomal subunits. *Proc. Natl. Acad. Sci. USA* **74:** 5547–5550.

Cusack, S. 1995. Eleven down and nine to go. *Nature Struct. Biol*. **2:** 824–831.

Czworkowski, J. and Moore, P. B. 1996. The elongation phase of protein synthesis. *Prog. Nucl. Acid Res. Mol. Biol.* **54:** 293–332.

Dabrowski, M., Spahn, C. M. T., and Nierhaus, K. H. 1995. Interaction of tRNAs with the ribosome at the A and P sites. *EMBO J*. **14:** 4872–4882.

Dabrowski, M., Spahn, C. M. T., Schäfer, M. A., and Nierhaus, K. H. 1998. Contact patterns of tRNAs do not change during ribosomal translocation. submitted.

Dennis, P. P. and Bremer, H. 1974. Differential rate of ribosomal protein synthesis in *Escherichia coli* B/r. *J. Mol. Biol.* **84:** 407–422.

Döring, T., Mitchell, P., Osswald, M., Bochkariov, D., and Brimacombe, R. 1994. The decoding region of 16S RNA: a cross-linking study of the ribosomal A, P and E sites using tRNA derivatized at position 32 in the anticodon loop. *EMBO J.* **13:** 2677–2685.

Echols, H. and Goodman M. F. 1991. Fidelity mechanism in DNA replication. *Annu. Rev. Biochem.* **60:** 477–511.

Eisenstein, M., Sharon, R., Berkovitch-Yellin, Z., Gewitz, H. S., Weinstein, S., Pebay-Peyroula, E., and Yonath, A. 1991. The interplay between X-ray crystallography, neutron diffraction, image reconstruction, organo-metallic chemistry and biochemistry in structural studies of ribosomes. *Biochimie* **73:** 879–886.

El'skaya, A. V., Ovcharenko, G. V., Palchevskii, S. S., Petrushenko, Z. M., Triana-Alonso, F. J., and Nierhaus, K. H. 1997. Three tRNA binding sites in rabbit liver ribosomes and the role of the intrinsic ATPase in 80S ribosomes from higher eukaryotes. *Biochemistry* **34**: 10492–10497.

Franceschi, F., Weinstein, S., Evers, U., Arndt, E., Jahn, W., Hansen, H. A. S., von Böhlen, K., Berkovitch-Yellin, Z., Eisenstein, M., Agmon, I., Thygesen, J., Volkmann, N., Bartels, H., Schlünzen, F., Zaytzev-Bashan, A., Sharon, R., Levin, I., Dribin, A., Sagi, I., Choli-Papadopoulou, T., Tsiboli, P., Kryger, G., Bennett, W. S., and Yonath, A. 1993. Toward atomic resolution of prokaryotic ribosomes: crystallographic, genetic and biochemical studies. **In:** *The Translational Apparatus—Structure, Function, Regulation, Evolution.* pp. 397–410. Nierhaus, K. H., Franceschi, F., Subramanian, A.R., Erdmann, V.A., and Wittmann-Liebold, B., Eds., Plenum Publishing Cooperation, New York.

Frank, J. 1996. *Three-Dimensional Electron Microscopy of Macromolecular Assemblies*. Academic Press, New York.

Frank, J., Verschoor, A., Radermacher, M., and Wagenknecht, T. 1990. Morphologies of eubacterial and eukaryotic ribosomes as determined by three-dimensional electron microscopy. **In:** *The Ribosome: Structure, Function and Evolution*. pp. 107–113. Hill, W. E., Dahlberg, A., Garrett, R. A., Moore, P. B., Schlessinger, D. and Warner, J. R., Eds., American Society for Microbiology, Washington, D.C.

Frank, J., Penczek, P., Grassucci, R., and Srivastava, S. 1991. Three-dimensional reconstruction of the 70S *Escherichia coli* ribosome in ice: The distribution of ribosomal RNA. *J. Cell Biol.* **115:** 597–605.

Frank, J., Verschoor, A., Li, Y., Zhu, J., Lata, R.K., Radermacher, M., Penczek, P., Grassucci, R., Agrawal, R.K., and Srivastava, S. 1995a. A model of the translational apparatus based on a three-dimensional reconstruction of the *Escherichia coli* ribosome. *Biochem. Cell Biol.* **73**: 757–765.

Frank, J., Zhu, J., Penczek, P., Li, Y., Srivastava, S., Verschoor, A., Radermacher, M., Grassucci, R., Lata, R. K., and Agrawal, R. K. 1995b. A model of protein synthesis based on cryo-electron microscopy of the *E. coli* ribosome. *Nature* **376:** 441–444.

Freistroffer, D. V., Pavlov, M. Y., MacDougall, J., Buckingham, R. H., and Ehrenberg, M. 1997. Release factor RF3 in *E. coli* accelerates the dissociation of release factor RF1 and RF2 from the ribosome in a GTP-dependent manner. *EMBO J.* **16**: 4126–4133.

Geigenmüller, U. and Nierhaus, K. H. 1990. Significance of the third tRNA binding site, the E site, on *E. coli* ribosomes for the accuracy of translation: an occupied E site prevents the binding of non-cognate tRNA. *EMBO J.* **9**: 4527–4533.

Girshovich, A. S., Bochkareva, E. S., and Vasiliev, V. D. 1986. Localization of elongation factor Tu on the ribosome. *FEBS Lett.* **197:** 192–198.

Gnirke, A. and Nierhaus, K. H. 1986. tRNA binding sites on the subunits of *Escherichia coli* ribosomes. *J. Biol. Chem*. **261:** 14506–14514.

Gnirke, A., Geigenmüller, U., Rheinberger, H.-J., and Nierhaus, K. H. 1989. The allosteric three-site model for the ribosomal elongation cycle—analysis with a heteropolymeric mRNA. *J. Biol. Chem.* **264:** 7291–7301.

Gornicki, P., Nurse, K., Heilmann, W. Boublik, M., and Ofengand, J. 1984. High resolution localization of the tRNA anticodon interaction site on the *Escherichia coli* 30S ribosomal subunit. *J. Biol. Chem.* **259:** 10493–10498.

Graifer, D. M., Nekhai, S. Y., Mundus, D. M., Fedorova, O. F., and Karpova, G. G. 1992. Interaction of human and *Escherichia coli* $tRNA^{Phe}$ with human 80S ribosomes in the presence of oligo- and polyuridylate templates. *Biochem. Biophys. Acta* **1171**: 56–67.

Grajevskaja, R. A., Ivanov, Y. V., and Saminsky, E. M. 1982. 70S ribosomes of *Escherichia coli* have an additional site for deacylated tRNA binding. *Eur. J. Biochem.* **128:** 47–52.

Grentzmann, G., Brechmier-Baey, D., Heurgue, V., Mora, L., and Buckingham, R. H. 1994. Localization and characterization of the gene encoding release factor RF3 in *Escherichia coli*. *Proc. Natl. Acad. Sci. USA* **91:** 5848–5852.

Grosjean D. H., DeHenau, S., and Crothers, D. M. 1978. On the physical basis for ambiguity in genetic coding interactions. *Proc. Natl. Acad. Sci. USA* **75:** 610–614.

Gualerzi, C. O., La Teana, A., Spurio, R., Canonaco, M. A., Severini, M., and Pon, C. L. 1990. Initiation of protein biosynthesis in prokaryotes: Recognition of mRNA by ribosomes and molecular basis for the function of initiation factors. **In:** *The Ribosome. Structure Function and Evolution*. pp. 281–291. Hill, W. E., Dahlberg, A., Garrett, R. A., Moore. P. B., Schlessinger, D., and Warner, J. R., Eds., American Society for Microbiology, Washington, D.C.

Hardesty, B., Odom, O.W., and Deng, H.-Y. 1986. The movement of tRNA through ribosomes during peptide elongation: The displacement model. **In:** *Structure, Function, and Genetics of Ribosomes*. pp. 47–67. Hardesty, B. and Kramer, G., Eds., Springer, New York.

Hartz, D., McPheeters, D. S., and Gold, L. 1990. From polynucleotide to natural mRNA translation initiation: function of *Escherichia coli* initiation factors. **In:** *The Ribosome: Structure, Function and Evolution.* pp. 275–280. Hill, W. E., Dahlberg, A., Garrett, R. A., Moore, P. B., Schlessinger, D., and Warner, J. R., Eds., American Society for Microbiology, Washington, D.C.

Hausner, T.-P., Geigenmüller, U., and Nierhaus, K. H. 1988. The allosteric three-site model for the ribosomal elongation cycle—new insights into the inhibition mechanisms of aminoglycosides, thiostrepton and viomycin. *J. Biol. Chem.* **263:** 13103–13111.

Hopfield, J. J. 1974. Kinetic Proofreading: A new mechanism for reducing errors in biosynthetic processes requiring high specificity. *Proc. Natl. Acad. Sci. USA* **71:** 4135–4139.

Horsfield, J. A., Wilson, D. N., Mannering, S. A., Adamski, F. M., and Tate, W. P. 1995. Prokaryotic ribosomes recode the HIV-1 gag-pol-1 frameshift sequence by an E/P site post-translocational simultaneous slippage mechanism. *Nucl. Acids Res.* **23:** 1487–1494.

Hubbard, J. M. and Hearst, J. E. 1991. Computer modeling 16S ribosomal RNA. *J. Mol. Biol.* **221:** 889–907.

Ibba, M., Curnow, A. W., and Söll, D. 1997. Aminoacyl-tRNA synthesis: divergent routes to a common goal. *Trends Biochem. Sci.* **22:** 39–42.

Janosi, L., Hara, H., Zhang, S., and Kaji, A. 1996. Ribosome recycling by ribosome recycling factor (RRF)—an important but overlooked step of protein biosynthesis. *Adv. Biophys.* **32:** 121–201.

Jelenc, P. C. and Kurland, C. G. 1979. Nucleoside triphosphate regeneration decreases the frequency of translation errors. *Proc. Natl. Acad. Sci. USA* **76:** 3174–3178.

Jünemann, R., Wadzack, J., Burkhardt, N., Schmitt, M., Zhao, J., Stuhrmann, H. B, and Nierhaus, K. H. 1997. Mapping the messenger RNA within the elongating ribosome. *Physica B* **234**: 193–195.

Kamekura, M., Hamana, K., and Matsuzaki, S. 1987. Polyamine contents and amino acid decarboxylation activities of extremely halophilic archaebacteria and some eubacteria. *FEMS Microbiol. Lett.* **43**: 301–305.

Kim, S. H., Quigley, G. J., Suddath, F. L., McPherson A., Sneden, D., Kim, J. J., Weinzierl, J., and Rich, A. 1972. Three-dimensional structure of yeast phenylalanine transfer RNA: Folding of polynucleotide chain. *Science* **179:** 285–288.

Kim, S. H., Suddath, F. L., Quigley, G. J., McPherson, A., Sussman, J. L., Wang, A. H. J., Seeman, N. C., and Rich, A. 1974. Three-dimensional tertiary structure of yeast phenylalanine transfer RNA. *Science* **185:** 435–440.

Kirillov, S. V. and Semenkov, Y. P. 1986. Extension of Watson's model for the elongation cycle of protein synthesis. *J. Biomol. Struct. Dynam.* **4:** 263–269.

Kirillov, S. V., Makarov, E. M., and Semenkov, Y. P. 1983. Quantitative study of interaction of deacylated tRNA with *Escherichia coli* ribosomes: role of 50S in formation of E-site. *FEBS Lett.* **157:** 91–94.

Knop, W., Hirai, M., Olah, G., Meerwinck, W., Schink, H.-J., Stuhrmann, H. B., Wagner, R., Wenkow-EsSouni, M., Zhao, J., Schärpf, O., Crichton, R. R., Krumpolc, M., Nierhaus, K. H., Niinikoski, T. O., and Rijllart, A. 1991. Polar-

ised neutron scattering from dynamic polarised targets in biology. *Physica B* **174:** 275–290.

Kurland, C. G., Jörgensen, F., Richter, A., Ehrenberg, M., Bilgin, N., and Rojas, A.-M. 1990. Through the accuracy window. **In:** *The Ribosome: Structure, Function and Evolution*. pp. 513–526. Hill, W. E., Dahlberg, A., Garrett, R. A., Moore. P. B., Schlessinger, D., and Warner, J. R., Eds., American Society for Microbiology, Washington, D.C.

Kutay, U., Spahn, C. M. T., and Nierhaus, K. H. 1990. Similarities and differences in the inhibition patterns of thiostrepton and viomycin: evidence for two functionally different populations of P sites when occupied with AcPhe-tRNA. *Biochim. Biophys. Acta* **1050:** 193–196.

Lake, J. A. 1977. Aminoacyl-tRNA binding at the recognition site is the first step of the elongation cycle of protein synthesis. *Proc. Natl. Acad. Sci. USA* **74:** 1903–1907.

Lata, K. R., Agrawal, R. K., Penczek, P., Grassucci, R., Zhu, J., and Frank, J. 1996. Three-dimensional reconstruction of the *Escherichia coli* 30S ribosomal subunit in ice. *J. Mol. Biol.* **262:** 43–52.

Leffers, H., Kjems, J., Ostergaard, L., Larsen, N., and Garrett, R. A. 1987. Evolutionary relationships amongst archaebacteria. A comparative study of 23S ribosomal RNAs of a sulfur-dependent extreme thermophile, an extreme halophile and a thermophilic methanogen. *J. Mol. Biol.* **195:** 43–61.

Lill, R. and Wintermeyer, W. 1987. Destabilization of codon-anticodon interaction in the ribosomal exit site. *J. Mol. Biol.* **196:** 137–148.

Lill, R., Robertson, J. M., and Wintermeyer, W. 1984. tRNA binding sites of ribosomes from *Escherichia coli. Biochemistry* **23:** 6710–6717.

Lill, R., Robertson, J. M., and Wintermeyer, W. 1986. Affinity of tRNA binding sites of ribosomes from *Escherichia coli. Biochemistry* **25:** 3245–3255.

Lill, R., Robertson, J. M., and Wintermeyer, W. 1989. Binding of the 3′ terminus of tRNA to 23S rRNA in the ribosomal exit site actively promotes translocation. *EMBO J.* **8:** 3933–3938.

Liljas, A., Ævarsson, A. Al-Karadaghi, S., Garber, M., Zheltonosova, J., and Brazhnikov, E. 1995. Crystallographic studies of elongation factor G. *Biochem. Cell Biol.* **73:** 1209–1216.

Lim, V. I. 1997. Analysis of interactions between the codon-anticodon duplexes within the ribosome: Their role in translation. *J. Mol. Biol.* **266**:877–890.

Lim, V. I. and Venclovas, C. 1992. Codon-anticodon pairing. A model for interacting codon-anticodon duplexes located at the ribosomal A- and P-sites. *FEBS Lett.* **313:** 133–137.

Lim, V., Venclovas, C., Spirin, A., Brimacombe, R., Mitchell, P., and Muller, F. 1992. How are tRNAs and mRNA arranged in the ribosome? An attempt to correlate the stereochemistry of the tRNA-mRNA interaction with constraints imposed by the ribosomal topography. *Nucl. Acids Res.* **20:** 2627–2537.

Lipmann, F. 1963. Messenger ribonucleic acid. *Prog. Nucl. Acid Res.* **1:** 135–161.

Lührmann, R., Eckard, H., and Stöffler, G. 1979. Codon-anticodon interaction at the ribosomal peptidyl-site. *Nature* **280:** 423–425.

Lusk, J. E., Williams, R. J. P., and Kennedy, E. P. 1968. Magnesium and the growth of *Escherichia coli*. *J. Biol. Chem.* **262:** 2618–2624.

Malhotra, A. and Harvey, S. C. 1994. A quantitative model of the *E. coli* 16S RNA in the 30S ribosomal subunit. *J. Mol. Biol*. **240:** 308–340.

May, R. P., Nowotny, V., Nowotny, P., Voss, H., and Nierhaus, K. H. 1992. Inter-protein distances within the large subunit from *Escherichia coli* ribosomes. *EMBO J*. **11:** 373–378.

Mesters, J. R., Potapov, A. P., de Graaf, J. M., and Kraal, B. 1994. Synergism between the GTPase activities of EF-Tu·GTP and EF-G·GTP on empty ribosomes. Elongation factors as stimulators of the ribosomal oscillation between two conformations. *J. Mol. Biol.* **242:** 644–654.

Mikuni, O., Ito, K., Moffat, J., Matsumura, K., McCaughan, K., Nobukuni, T., Tate, W., and Nakamura, Y. 1994. *Proc. Natl. Acad. Sci. USA* **91:** 5798–5802.

Mitchell, P., Osswald, M., Schüler, D., and Brimacombe, R. 1990. Selective isolation and detailed analysis of intra-RNA cross-links induced in the large ribosomal subunit of *Escherichia coli*: A model for the tertiary structure of the tRNA binding domain in 23S RNA. *Nucl. Acids Res.* **18:** 4325–4333.

Moazed, D. and Noller, H. F. 1986. Transfer RNA shields specific nucleotides in 16S ribosomal RNA from attack by chemical probes. *Cell* **47:** 985–994.

Moazed, D. and Noller, H. F. 1989a. Interaction of tRNA with 23S rRNA in the ribosomal A, P, and E sites. *Cell* **57**: 585–597.

Moazed, D. and Noller, H. F. 1989b. Intermediate states in the movement of tRNA in the ribosome. *Nature* **342:** 142–148.

Moazed, D. and Noller, H. F. 1990. Binding of tRNA to the ribosomal A and P sites protects two distinct sets of nucleotides in 16S rRNA. *J. Mol. Biol.* **211:** 135–145.

Möller, A., Wild, U., Riesner, D., and Gassen, H. C. 1979. Evidence from ultraviolet absorbance measurements for a codon-induced conformational change in lysine tRNA from *Escherichia coli*. *Proc. Natl. Acad. Sci. USA* **76:** 3266–3270.

Nierhaus, K. H. 1990. The allosteric three-site model for the ribosomal elongation cycle: features and future. *Biochemistry* **29:** 4997–5008.

Nierhaus, K. H. 1993. Solution of the ribosomal riddle: how the ribosome selects the correct aminoacyl-tRNA out of 41 similar contestants. *Mol. Microbiol.* **9:** 661–669.

Nierhaus, K. H. 1996. An elongation factor turn-on. *Nature* **379**: 491–492.

Nierhaus, K. H., Lietzke, R., Nowotny, V., Schulze, H., Wurmbach, P., Stuhrmann, H. B., and May, R. P. 1983. Shapes of and distances between components within the large (50S) subunit of *E.coli* ribosomes. *Physica B* **120:** 426–435.

Nierhaus, K. H., Beyer, D., Dabrowski, M., Schäfer, M. A., Spahn, C. M. T., Wadzack, J., Bittner, J.-U., Burkhardt, N., Diedrich, G., Jünemann, R., Kamp, D., Voss, H., and Stuhrmann H. B. 1995. The elongating ribosome: structural and functional aspects. *Biochem. Cell Biol.* **73**: 1011–1021.

Nierhaus, K. H., Wadzack, J., Burkhardt, N., Jünemann, R., Meerwinck, W., Willumeit, R., and Stuhrmann, H. B. 1998. Structure of the elongating ribosome: arrangement of the two tRNAs before and after translocation. *Proc. Natl. Acad. Sci. USA* **95:** 945–950.

Nierhaus, K. H., Jünemann, R., and Spahn C. M. T. 1997. Are the current three-site models valid descriptions of the ribosomal elongation cycle? *Proc. Natl. Acad. Sci. USA* **94:** 10499–10500.

Ninio, J. 1974. A Semi-quantitative treatment of missense and nonsense suppression in the strA and ram ribosomal mutants of *Escherichia coli*—evaluation of some molecular parameters of translation in *vivo*. *J. Mol. Biol.* **84:** 297–313.

Ninio, J. 1975. Kinetic amplification of enzyme discrimination. *Biochimie* **57:** 587–595.

Nissen, P., Kjeldgaard, M., Thirup, S., Polekhina, G., Reshetnikova, L., Clark, B. F. C., and Nyborg, J. 1995. Crystal structure of the ternary complex of Phe-tRNA^{Phe}, EF-Tu, and a GTP analog. *Science* **270:** 1464–1472.

Noller, H. F. 1991. Ribosomal RNA and translation. *Annu. Rev. Biochem.* **60:** 191–227.

Noller, H. F., Moazed, D., Stern, S., Powers, T., Allen, P. N., Robertson, J. M., Weiser, B., and Triman, K. 1990. Structure of rRNA and its functional interactions in translation. **In:** *The Ribosome: Structure, Function and Evolution.* pp. 73–92. Hill, W. E., Dahlberg, A., Garrett, R. A., Moore, P. B., Schlessinger, D. and Warner, J. R., Eds., American Society for Microbiology, Washington, D.C.

Oakes, M., Henderson, E., Scheinman, A., Clark, M., and Lake, J. A. 1986. Ribosome structure, function, and evolution: mapping ribosomal RNA, proteins, and functional sites in three dimensions. **In:** *Structure, Function, and Genetics of Ribosomes*. pp. 47–67. Hardesty, B. and Kramer, G., Eds., Springer, New York.

O'Connor, M., Willis, N. M., Bossi, L., Gesteland, R. F., and Atkins J. F. 1993. Functional tRNAs with altered 3′ends. *EMBO J.* **13:** 2559–2566.

Ofengand, J. and Liou, R. 1981. Correct codon-anticodon base pairing at the 5′-anticodon position

blocks covalent cross-linking between transfer ribonucleic acid and 16S RNA at the ribosomal P site. *Biochemistry* **20:** 552–559.

Olson, H. M., Grant, P. G., Cooperman, B. S., and Glitz, D. G. 1982. Immunoelectron microscopic localization of puromycin binding on the large subunit of the *Escherichia coli* ribosome. *J. Biol. Chem.* **257:** 2649–2656.

Olson, H. M., Nicholson, A. W., Cooperman, B. S., and Glitz, D. G. 1985. Localization of sites of photoaffinity labeling of the large subunit of the *Escherichia coli* ribosomes by arylazide derivative of puromycin. *J. Biol. Chem.* **260:** 10326–10331.

Olson, H. M., Lasater, L. S., Cann, P. A., and Glitz, D. G. 1988. Messenger RNA orientation on the ribosome: placement by electron microscopy of antibody-complementary oligodeoxynucleotide complexes. *J. Biol. Chem.* **263:** 15196–15204.

Paulsen, H. and Wintermeyer, W. 1986. tRNA topography during translocation: steady-state and kinetic fluorescence energy-transfer studies. *Biochemistry* **25:** 2749–2756.

Pavlov, M. Y., Freistroffer, D. V., MacDougall, J., Buckingham, R. H., and Ehrenberg, M. 1997. Fast recycling of *Escherichia coli* ribosomes requires both ribosome recycling factor (RRF) and release factor RF3. *EMBO J.* **16**: 4134–4141.

Peters, M. and Yarus, M. 1979. Transfer RNA selection at the ribosomal A and P sites. *J. Mol. Biol.* **134:** 471–491.

Podkowinski, J. and Gornicki, P. 1989. Ribosomal proteins S7 and L1 are located close to the decoding site of *E. coli* ribosome—affinity labeling studies with modified tRNAs carrying photoreactive probes attached adjacent to the 3′-end of the anticodon. *Nucl. Acids Res.* **17:** 8767–8782.

Potapov, A. P. 1982. A stereospecific mechanism for the aminoacyl-tRNA selection at the ribosome. *FEBS Lett.* **146:** 28–33.

Potapov, A. P., Triana-Alonso, F. J., and Nierhaus, K. H. 1995. Ribosomal decoding processes at codons in the A or P sites depend differently on 2′-OH groups. *J. Biol. Chem.* **270:** 17680–17684.

Powers, T. and Noller, H. F. 1994a. Selective perturbation of G530 of 16S rRNA by translational miscoding agents and a streptomycin-dependence mutation in protein S12. *J. Mol. Biol.* **235:** 156–172.

Powers, T. and Noller, H. F. 1994b. The 530 loop of 16S rRNA: a signal to EF-Tu? *Trends Genet.* **10:** 27–31.

Remme, J., Margus, T., Villems, R., and Nierhaus, K. H. 1989. The third tRNA-binding site, the E site, is occupied in native polysomes. *Eur. J. Biochem*. **183:** 281–284.

Rheinberger, H.-J. 1991. The function of the translating ribosome: allosteric three-site model of elongation. *Biochimie* **73:** 1067–1088.

Rheinberger, H.-J. and Nierhaus, K. H. 1980. Simultaneous binding of three tRNA molecules by the ribosome of *Escherichia coli*. *Biochem. Int.* **1:** 297–303.

Rheinberger, H.-J. and Nierhaus, K. H. 1983. Testing an alternative model of the ribosomal peptide elongation cycle. *Proc. Natl. Acad. Sci. USA* **80:** 4213–4217.

Rheinberger, H.-J. and Nierhaus, K. H. 1986a. Allosteric interactions between the ribosomal transfer RNA-binding sites A and E. *J. Biol. Chem.* **261:** 9133–9139.

Rheinberger, H.-J. and Nierhaus, K. H. 1986b. Adjacent codon-anticodon interactions of both tRNAs present at the ribosomal A and P or P and E sites. *FEBS Lett.* **204:** 97–99.

Rheinberger, H.-J. and Nierhaus, K. H. 1987. The ribosomal E site at low Mg^{2+}: coordinate inactivation of ribosomal functions at Mg^{2+} concentrations below 10 m*M* and its prevention by polyamines. *J. Biomol. Struct. Dyn.* **5:** 435–446.

Rheinberger H.-J., Sternbach, H., and Nierhaus, K. H. 1981. Three tRNA binding sites on *Escherichia coli* ribosomes. *Proc. Natl. Acad. Sci. USA* **78:** 5310–5314.

Rheinberger H.-J., Sternbach, H., and Nierhaus, K. H. 1986. Codon-anticodon interaction at the ribosomal E site. *J. Biol. Chem.* **261:** 9140–9143.

Rheinberger, H.-J., Geigenmüller, U., Wedde, M., and Nierhaus, K. H. 1988. Parameters for the preparation of *Escherichia coli* ribosomes and

ribosomal subunits active in tRNA binding. *Meth. Enzymol.* **164:** 658–670.

Rich, A. 1974. How transfer RNA may move inside the ribosome. **In**: *Ribosomes.* pp. 871–884. Nomura, M., Tissières, A., and Lengyel, P., Eds., Cold Spring Harbor Press, New York.

Rinke-Appel, J., Jünke, N., Brimacombe, R., Lavrik, I., Dokudovskaya, S., Dontsova, O., and Bogdanov, A. 1994. Contacts between 16S ribosomal RNA and mRNA, within the spacer region separating the AUG initiator codon and the Shine-Dalgarno sequence; a site-directed cross-linking study. *Nucl. Acids. Res.* **22:** 3018–3025.

Rinke-Appel, J., Jünke, N., Osswald, M., and Brimacombe, R. 1995. The ribosomal environment of tRNA: crosslinks to rRNA from positions 8 and 20:1 in the central fold of tRNA located at the A, P, or E site. *RNA* **1:** 1018–1028.

Robertson, J. M. and Wintermeyer, W. 1987. Mechanism of ribosomal translocation—tRNA binds transiently to an exit site before leaving the ribosome during translocation. *J. Mol. Biol.* **196:** 525–540.

Robertson, J. M., Lill, R., and Wintermeyer, W. 1984. Elongation factor G induced release of tRNA during ribosomal translocation. In: *Metabolism and Enzymology of Nucleic Acids Including Gene Manipulations*. pp. 307–319. Zelinka, J. and Balan, J., Eds., Publishing House of the Slovac Academy of Science, Bratislava, Czechoslovakia.

Robertson, J. M., Paulsen, H., and Wintermeyer, W. 1986. Pre-steady-state kinetics of ribosomal translocation. *J. Mol. Biol.* **192:** 351–360.

Robertus, J. D., Ladner, J. E., Finch, L. T., Rhodes, D., Brown, R. S., Clark, B. F. C., and Klug, A. 1974. Structure of yeast phenylalanine tRNA at 3 Å resolution. *Nature* **250:** 546–551.

Rodnina, M. V. and Wintermeyer, W. 1992. Two tRNA-binding sites in addition to A and P sites on eukaryotic ribosomes. *J. Mol. Biol.* **228**: 450–459.

Rodnina, M. V. and Wintermeyer, W. 1995. GTP consumption of elongation factor Tu during translation of heteropolymeric mRNAs. *Proc. Natl. Acad. Sci. USA* **92:** 1945–1949**.**

Rodnina, M. V., El'skaya, A. V., Semenkov, Y. P., and Kirillov, S. V. 1988. Number of tRNA binding sites on 80S ribosomes and their subunits. *FEBS Lett.* **231:** 71–74.

Rodnina, M. V., Fricke, R., Kuhn, L., and Wintermeyer, W. 1995. Codon-dependent conformational change of elongation factor Tu proceeding GTP hydrolysis on the ribosome. *EMBO J.* **14:** 2613–2619.

Saruyama, H. and Nierhaus, K. H. 1986. Evidence that the three-site model for the ribosomal elongation cycle is also valid in the archaebacterium *Halobacterium halobium. Mol. Gen. Genet.* **204:** 221–228.

Schatz, D., Leberman, R., and Eckstein, F. 1991. Interaction of *Escherichia coli* $tRNA^{Ser}$ with its cognate aminoacyl-tRNA synthetase as determined by footprinting with phosphorothioate-containing tRNA transcripts. *Proc. Natl. Acad. Sci. USA* **88**: 6132–6136.

Schilling-Bartetzko, S., Franceschi, F., and Nierhaus, K.H. 1992a. Apparent association constants of tRNAs for the ribosomal A, P, and E sites. *J. Biol. Chem.* **267**: 4693–4702.

Schilling-Bartetzko, S., Bartetzko, A., and Nierhaus, K.H. 1992b. Kinetic and thermodynamic parameters for tRNA binding and for the translocation reaction. *J. Biol. Chem.* **267**: 4703–4712.

Semenkov, Y. P., Rodnina, M. V., and Wintermeyer, W. 1996. The allosteric three-site model of elongation cannot be confirmed in a well-defined ribosome system from *Escherichia coli*. *Proc. Natl. Acad. Sci. USA* **93:** 12183–12188.

Semenkov, Y. P., Shapkina, T. G., and Kirillov, S. V. 1992. Puromycin reaction of the A-site bound peptidyl-tRNA. *Biochimie* **74:** 411–417.

Sergiev, P. V., Lavrik, I. N., Wlasoff, V. A., Dokudovskaya, S. S., Dontsova, O. A., Bogdanov, A. A., and Brimacombe, R. 1997. The path of mRNA through the bacterial ribosome: a site-directed crosslinking study using new photoreactive derivatives of guanosine and uridine. *RNA* **3:** 464–475.

Spahn, C. M. T. and Prescott, C. D. 1996. Throwing a spanner in the works: antibiotics and the

translational apparatus. *J. Mol. Med.* **74:** 423–439.

Spirin, A. S. 1983. Location of tRNA on the ribosome. *FEBS Lett.* **156:** 217–221.

Spirin, A. S. 1985. Ribosomal translocation: facts and models. *Prog. Nucl. Acid Res. Mol. Biol.* **32:** 75–114.

Stark, H., Mueller, F., Orlova, E. V., Schatz, M., Dube, P., Erdemir, T., Zemlin, F., Brimacombe, R., and v. Heel, M. 1995. The 70S *Escherichia coli* ribosome at 23 Å resolution: fitting the ribosomal RNA. *Structure* **3:** 815–821.

Stark, H., Orlova, E. V., Rinke-Appel, J., Jünke, N., Mueller, F., Rodnina, M., Wintermeyer, W., Brimacombe, R., and v. Heel, M. 1997. Arrangement of tRNAs in pre- and post-translocational ribosomes revealed by electron cryomicroscopy. *Cell* **88**: 19–28.

Stern, S., Weiser, B., and Noller, H. F. 1988. Model for the three-dimensional folding of 16S ribosomal RNA. *J. Mol. Biol.* **204:** 447-481.

Stöffler, G. and Stöffler-Meilicke, M. 1986. Immuno electron microscopy on *Escherichia coli* ribosomes. **In:** *Structure, Function, and Genetics of Ribosomes*. pp. 28–46. Hardesty, B. and Kramer, G., Eds., Springer, New York.

Stöffler-Meilicke, M., and Stöffler, G. 1990. Topography of the ribosomal proteins from *Escherichia coli* within the intact subunits as determined by immunoelectron microscopy and protein-protein cross-linking. **In:** *The Ribosome: Structure, Function and Evolution*. pp. 123–133. Hill, W. E., Dahlberg, A., Garrett, R. A., Moore, P. B., Schlessinger, D., and Warner, J. R., Eds., American Society for Microbiology, Washington, D.C.

Stuhrmann, H. B. 1989. Methods on isotopic and spin contrast variation. *Physica B* **156/157:** 444–451.

Stuhrmann, H. B. 1991. Frozen spin targets in ribosomal structure research. *Biochimie* **73:** 899–913.

Stuhrmann, H. B., Koch, M. H. J., Parfait, R., Haas, J., Ibel, K., and Crichton, R. R. 1977. Shape of the 50S subunit of *Escherichia coli* ribosomes. *Proc. Natl. Acad. Sci. USA* **74:** 2316–2320.

Stuhrmann, H. B., Koch, M. H. J., Haas, J., Ibel, K., and Crichton, R. R. 1978. Determination of the distribution of protein and nucleic acid in the 70S ribosomes of *Escherichia coli* and their 30S subunits by neutron scattering. *J. Mol. Biol.* **119:** 203–212.

Stuhrmann, H.B., Burkhardt, N., Diedrich, G., Jünemann, R., Meerwinck, W., Schmitt, M., Wadzack, J., Willumeit, R., Zhao, J., and Nierhaus, K.H. 1995. Proton- and deuteron spin targets in biological structure research. *Nucl. Instr. Meth. Phys. Res. A* **356:** 124–132.

Sundaralingam, M., Brennan, T. Yathindra, N., and Ichikawa, T. 1975. Stereochemistry of messenger RNA (codon) and transfer RNA (anticodon) interaction on the ribosome during peptide bond formation. **In**: *Structure and Conformation of Nucleic Acids and Protein-Nucleic Acid Interactions.* pp. 101–115. Sundaralingam, M. and Rao, S. T., Eds., University Park Press, Baltimore.

Svergun, D. I., Koch, M. H. J., and Serdyuk, I. N. 1994a. Structural model of the 50S subunit of *Escherichia coli* ribosomes from solution scattering: I. X-ray synchrotron radiation study. *J. Mol. Biol.* **240:** 66–77.

Svergun, D. I., Koch, M. H. J., Pedersen, J. S., and Serdyuk, I. N. 1994b. Structural model of the 50S subunit of *Escherichia coli* ribosomes from solution scattering: II. neutron scattering study. *J. Mol. Biol.* **240:** 78–86.

Svergun, D. I., Pedersen, J. S., Serdyuk, I. N., and Koch, M. H. J. 1994c. Solution scattering from 50S ribosomal subunit resolves inconsistency between electron microscopic models. *Proc. Natl. Acad. Sci. USA* **91:** 11826–11830.

Svergun, D. I., Burkhardt, N., Pedersen, J. S., Koch, M. H. J., Volkov, V. V., Kozin, M. B., Meerwinck, W., Stuhrmann, H. B., Diederich, G., and Nierhaus, K. H. 1997a. Structural analysis of the 70S *E. coli* ribosome and its RNA by solution scattering. I. Invariants and validation of electron microscopic models. *J. Mol. Biol.* **271**: 588–601.

Svergun, D. I., Burkhardt, N., Pedersen, J. S., Koch, M. H. J., Volkov, V. V., Kozin, M. B., Meerwinck, W., Stuhrmann, H. B., Diederich, G., and Nierhaus, K. H. 1997b. Structural analysis of the 70S *E. coli* ribosome and its RNA by solution scattering. II. Model building. *J. Mol. Biol.* **271**: 602–618.

Tabor, C. W. and Tabor, H. 1985. Polyamines in microorganisms. *Microbiol. Rev.* **49:** 81–99.

Tate, W. P. and Brown, C. M. 1992. Translational termination: "stop" for protein synthesis or "pause" for regulation of gene expression. *Biochemistry* **31:** 2443–2450.

Traut, R. R. and Monroe, R. E. 1964. The puromycin reaction and its relation to protein synthesis. *J. Mol. Biol.* **11:** 63–72.

Triana, F. J., Nierhaus, K. H., Ziehler, J., and Chakraburtty, K. 1993. Defining the function of EF-3, a unique elongation factor in low fungi. **In:** *The Translational Apparatus: Structure, Function, Regulation, Evolution.* pp. 327–338. Nierhaus, K. H., Franceschi, F., Subramanian, A. R., Erdmann, V.A., and Wittmann-Liebold, B., Eds., Plenum Press, New York.

Triana-Alonso, F. J., Chakraburtty, K., and Nierhaus, K. H. 1995. The elongation factor 3 unique in higher fungi and essential for protein biosynthesis is an E site factor. *J. Biol. Chem.* **270:** 20743–20748.

Urlaub, H., Kruft, V., Bischof, O., Müller, E.-C., and Wittmann-Liebold, B. 1995. Protein-rRNA binding features and their structural and functional implications in ribosomes as determined by cross-linking studies. *EMBO J.* **14:** 4578–4588.

Vasiliev, V. D., Selinova, O. M., Baranov, V. I., and Spirin, A. S. 1983. Structural study of translating 70S ribosomes from *Escherichia coli*. *FEBS Lett.* **155:** 167–172.

Wadzack, J., Burkhardt, N., Jünemann, R., Diedrich, G., Nierhaus, K. H., Frank, J., Penczek, P., Meerwinck, W., Schmitt, M., Willumeit, R., and Stuhrmann, H. B. 1997. Direct localization of the tRNAs within the elongating ribosome by means of neutron scattering (proton-spin contrast-variation). *J. Mol. Biol.* **266**: 343–356.

Walleczek, J., Schüler, D., Stöffler-Meilicke, M., Brimacombe, R., and Stöffler, G. 1988. A model of the spatial arrangement of the proteins in the large subunit of the *Escherichia coli* ribosome. *EMBO J.* **7:** 3571–3576.

Watson, J. D. 1963. Involvement of RNA in the synthesis of proteins. *Science* **140:** 17–26.

Watson, J. D. 1964. The synthesis of proteins after ribosomes. *Bull. Soc. Chim. Biol.* **46:**1399–1425.

Wettstein, F. O. and Noll, H. 1965. Binding of transfer ribonucleic acid to ribosomes engaged in protein synthesis: number and properties of ribosomal binding sites. *J. Mol. Biol.* **11:** 35–53.

Wintermeyer, W. and Robertson, J. M. 1982. Transient kinetics of transfer ribonucleic acid binding to the ribosomal A and P sites: observation of a common intermediate complex. *Biochemistry* **21:** 2246–2252.

Wintermeyer, W., Lill, R., and Robertson, J. M. 1990. Role of the tRNA Exit Site in Ribosomal Translocation. **In:** *The Ribosome: Structure, Function and Evolution*. pp. 348–357. Hill, W. E., Dahlberg, A., Garrett, R. A., Moore. P. B., Schlessinger, D., and Warner, J. R., Eds., American Society for Microbiology, Washington, D.C.

Wittmann H. G. 1986. Structure of ribosomes. **In:** *Structure, Function, and Genetics of Ribosomes*. pp. 1–27. Hardesty, B. and Kramer, G., Eds., Springer, Berlin.

Wittmann-Liebold, B., Köpke, A. K. E., Arndt, E., Krömer, W., Hatakeyama, T., and Wittmann, H. G. 1990. Sequence comparison and evolution of ribosomal proteins and their genes. **In:** *The Ribosome: Structure, Function and Evolution*. pp. 598–616. Hill, W. E., Dahlberg, A., Garrett, R. A., Moore. P. B., Schlessinger, D., and Warner, J. R., Eds., American Society for Microbiology, Washington, D.C.

Wower, J., Hixson, S. S., and Zimmermann, R. A. 1989. Labeling the peptidyltransferase center of the *Escherichia coli* ribosome with photoreactive $tRNA^{Phe}$ derivatives containing azidoadenosine at the 3¢ end of the acceptor arm: a model of the tRNA-ribosome complex. *Proc Natl. Acad. Sci USA* **86:** 5232–5236.

Wower, J. and Zimmermann, R. A. 1991. A consonant model of the tRNA-ribosome complex during the elongation cycle of translation. *Biochimie* **73**: 961–969.

Wower, J., Scheffer, P., Sylvers, L. A., Wintermeyer, W., and Zimmermann, R. A. 1993a. Topography of the E site on the *E. coli* ribosome. *EMBO J.* **12:** 617–623.

Wower, J., Sylvers, L. A., Rosen, K. V., Hixson, S. S., and Zimmermann, R. A. 1993b. A model of the tRNA binding sites on the *Escherichia coli* ribosome. **In:** *The Translational Apparatus—Structure, Function, Regulation, Evolution*. pp. 455–464. Nierhaus, K. H., Franceschi, F., Subramanian, A.R., Erdmann, V.A., and Wittmann-Liebold, B., Eds., Plenum Publishing Cooperation, New York.

Wower, J., Rosen, K. V., Hixson, S. S., and Zimmermann, R. A. 1994. Recombinant photoreactive tRNA molecules as probes for cross-linking studies. *Biochimie* **76:** 1235–1246.

Wower, J., Wower, I. K., Kirillov, S. V., Rosen; K. V., Hixson, S. S., and Zimmermann, R. A. 1995. Peptidyl transferase and beyond. *Biochem. Cell Biol.* **73:** 1041–1047.

Wurmbach, P. and Nierhaus, K. H. 1979. Codon-anticodon interaction at the ribosomal P (peptidyl-tRNA) site. *Proc. Natl. Acad. Sci. USA* **76:** 2143–2147.

Zhu, J., Penczek, P. A., Schröder, R., and Frank, J. 1997. Three-dimensional reconstruction with contrast tranfer function correction from energy-filtered cryoelectron micrographs: procedure and application to the 70S *Escherichia coli* ribosome. *J. Struc. Biol.* **118**: 197–219.